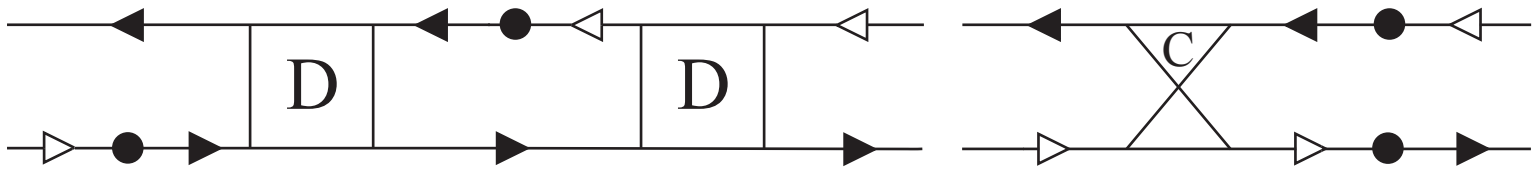


QUANTUM COHERENCE AND MESOSCOPIC FLUCTUATIONS

Markku Stenberg



Helsinki University of Technology

Laboratory of Physics

Espoo 2007

QUANTUM COHERENCE AND MESOSCOPIC FLUCTUATIONS

Markku Stenberg

Dissertation for the degree of Doctor of Science in Technology to be presented with due permission of the Department of Engineering Physics and Mathematics for public examination and debate in Auditorium F1 at Helsinki University of Technology (Espoo, Finland) on the 7th of September, 2007, at 12 o'clock noon.

Helsinki University of Technology

Department of Engineering Physics and Mathematics

Laboratory of Physics

Teknillinen korkeakoulu

Teknillisen fysiikan ja matematiikan osasto

Fysiikan laboratorio

Dissertations of Laboratory of Physics, Helsinki University of Technology
ISSN 1455-1802

Dissertation 149 (2007):

Markku Stenberg: Quantum coherence and mesoscopic fluctuations

ISBN 978-951-22-8874-8 (print)

ISBN 978-951-22-8875-5 (electronic)

URL: <http://lib.ttk.fi/Diss/2007/isbn9789512288755>

© Markku Stenberg

Multiprint Oy/Otamedia

Espoo 2007



HELSINKI UNIVERSITY OF TECHNOLOGY P. O. BOX 1000, FI-02015 TKK http://www.tkk.fi		ABSTRACT OF DOCTORAL DISSERTATION	
Author Stenberg, Markku Pertti Valfrid			
Name of the dissertation Quantum coherence and mesoscopic fluctuations			
Date of manuscript 10.5.2007		Date of the dissertation 7.9.2007	
<input type="checkbox"/> Monograph		<input checked="" type="checkbox"/> Article dissertation (summary + original articles)	
Department Department of Engineering Physics and Mathematics			
Laboratory Laboratory of Physics			
Field of research Theoretical condensed-matter physics			
Opponent(s) Prof. Wolfgang Belzig			
Supervisor (Instructor) Acad. Prof. Risto Nieminen			
Abstract <p>At low temperatures submicron-size structures may exhibit certain distinctive quantum features. These include, e.g., quantum interference effects, many-body correlation effects and different collective phenomena. At the borderline of the microscopic and macroscopic world resides a regime which is called mesoscopic. Mesoscopic systems are small enough to exhibit quantum coherent behavior, yet they contain a sufficiently large number of particles to allow a statistical description. Mesoscopic conductors may be considered as a realistic platform for information processing and future nanoelectronics since they allow for scalability and integration to larger circuits.</p> <p>The charge transfers through disordered mesoscopic conductors exhibit different kinds of variations referred as mesoscopic fluctuations, e.g., noise, universal conductance fluctuations, and higher-order fluctuations. Containing information on the physics of the transport phenomenon not contained in conductance, these phenomena provide a delicate way to probe quantum coherence in disordered structures. Moreover, mesoscopic fluctuations can be used as a test bench for conventional condensed matter theories. In this Thesis, mesoscopic fluctuations are studied in order to extend the existing theories for the fluctuation point of view, for example, for the superconducting proximity effect, reflectionless tunneling, and weak localization.</p> <p>When a normal metal is in contact with a superconductor, the superconducting proximity effect induces coherent correlations of electrons and holes in the former. Studying shot noise indicates that, in addition, the proximity effect induces anticorrelations between different electron-hole pairs in a normal metal. In this Thesis, for example, noise correlations in phase coherent normal-superconducting structures are investigated. In normal metals, weak localization behavior is considered. For example, a novel scaling relation for cumulants characterizing conductance fluctuations is found.</p> <p>The quantum coherent phenomena considered in this Thesis have been studied by using three different kinds of theoretical approaches: the quasiclassical Keldysh Green's function formalism, the random matrix theory, and a numerical scattering approach.</p>			
Keywords mesoscopics, phase coherence, full counting statistics, superconductivity, proximity effect			
ISBN (printed) 978-951-22-8874-8		ISSN (printed) 1455-1802	
ISBN (pdf) 978-951-22-8875-5		ISSN (pdf)	
ISBN (others)		Number of pages 122	
Publisher Multiprint Oy/Otamedia			
Print distribution Laboratory of Physics, Helsinki University of Technology			
<input checked="" type="checkbox"/> The dissertation can be read at http://lib.tkk.fi/Diss/2007/isbn9789512288755/			



VÄITÖSKIRJAN TIIVISTELMÄ		TEKNILLINEN KORKEAKOULU PL 1000, 02015 TKK http://www.tkk.fi	
Tekijä Stenberg, Markku Pertti Valfrid			
Väitöskirjan nimi Quantum coherence and mesoscopic fluctuations			
Käsikirjoituksen päivämäärä 10.5.2007		Korjatun käsikirjoituksen päivämäärä 14.8.2007	
Väitöstilaisuuden ajankohta 7.9.2007			
<input type="checkbox"/> Monografia		<input checked="" type="checkbox"/> Yhdistelmäväitöskirja (yhteenveto + erillisartikkelit)	
Osasto Teknillisen fysiikan ja matematiikan osasto Laboratorio Fysiikan laboratorio Tutkimusala Teoreettinen kondensoituneen aineen fysiikka Vastaväittäjä(t) prof. Wolfgang Belzig Työn valvoja akat. prof. Risto Nieminen Työn ohjaaja			
Tiivistelmä <p>Matalissa lämpötiloissa riittävän pienten rakenteiden kvanttimekaaniset koherentit ominaisuudet nousevat esiin. Tällaisia ovat esimerkiksi kvantti-interferenssi-, monihiukkas- ja erilaiset kollektiiviset ilmiöt. Mikroskooppisen ja makroskooppisen maailman välissä sijaitsee mesoskooppiseksi kutsuttu alue. Mesoskooppiset systeemit ovat tarpeeksi pieniä, jotta kvanttikoherentteja ilmiötä voi esiintyä. Toisaalta ne sisältävät riittävästi hiukkasia tilastollisen kuvauksen kannalta. Mesoskooppisten johteiden voidaan odottaa soveltuvan tulevaisuuden nanoelektronikan käyttöön, sillä niistä koostuvia komponentteja on mahdollista liittää yhteen suuremmiksi virtapiireiksi.</p> <p>Epäjärjestyneissä mesoskooppisissa johteissa kuljetusilmiöitä kuvaavat suureet vaihtelevat aika- ja ensemble-keskiarvojen ympärillä. Nämä mesoskooppisiksi fluktuatioiksi kutsutut ilmiöt sisältävät informaatiota, jota ei ole esimerkiksi keskiarvoistetussa johtavuudessa. Tässä väitöskirjassa laajennetaan aiempia teorioita käsittelemään mesoskooppisia fluktuatioita, esimerkiksi suprajohtavan läheisilmiön, heijastumattoman tunneloinnin ja heikon lokalisaation ilmiön yhteydessä. Joissakin tapauksissa mesoskooppiset fluktuatiot tarjoavat myös uuden tavan testata olemassa olevia kondensoituneen aineen fysiikan teorioita.</p> <p>Suprajohteessa kiinni olevaan normaalimetalliin indusoituu suprajohtavan läheisilmiön vaikutuksesta elektronien ja aukkojen koherentteja korrelaatioita. Ns. raekohinan tutkiminen näyttää, että tämän lisäksi läheisilmiö indusoi normaalimetalliin erillisten elektroni-aukko -parien välisiä antikorrelaatioita. Tässä työssä on tutkittu esimerkiksi virran raekohinaa vaihekoherentteissa normaali-suprajohtavissa rakenteissa. Normaalimetalleissa on tarkasteltu esimerkiksi heikon lokalisaation ilmiötä, johon liittyen löydetään konduktanssifluktuatioita kuvaaville kumulanteille uusi skaalauslaki.</p> <p>Kvanttikohherentteja ilmiötä on tässä työssä tutkittu käyttäen kolmea erilaista teoreettista lähestymistapaa: kvasiklassista Keldysh Greenin funktio -formalismia, satunnaisten matriisien teoriaa sekä numeerista sirontalähestymistapaa.</p>			
Asiasanat mesoskopia, vaihekoherenssi, laskentastatistiikka, suprajohtavuus, läheisilmiö			
ISBN (painettu) 978-951-22-8874-8		ISSN (painettu) 1455-1802	
ISBN (pdf) 978-951-22-8875-5		ISSN (pdf)	
Kieli englanti		Sivumäärä 122	
Julkaisija Multiprint Oy/Otamedia			
Painetun väitöskirjan jakelu Fysiikan laboratorio, Teknillinen Korkeakoulu			
<input checked="" type="checkbox"/> Luettavissa verkossa osoitteessa http://lib.tkk.fi/Diss/2007/isbn9789512288755/			

Affiliation

Author

Markku Stenberg
Laboratory of Physics
Helsinki University of Technology
Espoo, Finland

Supervisor

Acad. Prof. Dr. Risto Nieminen
Laboratory of Physics
Helsinki University of Technology
Espoo, Finland

Opponent

Prof. Dr. Wolfgang Belzig
Department of Physics
University of Konstanz
Konstanz, Germany

Reviewer

Dr. Peter Samuelsson
Division of Mathematical Physics
Department of Physics
Lund University
Lund, Sweden

Reviewer

Prof. Dr. Antti-Pekka Jauho
MIC – Department of Micro and Nanotechnology
Technical University of Denmark
Lyngby, Denmark

Preface

THE research for this Thesis has been carried out in the Materials Physics Laboratory and in the Laboratory of Physics at the Helsinki University of Technology. I wish I could thank Prof. Martti Salomaa, the director of the Materials Physics Laboratory, for the opportunity to begin this work. Martti untimely passed away in December 2004. I would like to acknowledge Prof. Pekka Hautojärvi, Acad. Prof. Risto Nieminen, and also Dr. Sami Virtanen for taking care of the practical issues in the Laboratory in the months that followed. I extend thanks to Risto, the supervisor of this Thesis, and Pekka for providing excellent working conditions for research.

On the scientific side, I would, first of all, like to thank Tero Heikkilä for nice and useful discussions as well as helping me with the finishing of the present manuscript. I wish also to express my gratitude to my other coauthors, Ari Alastalo, Colin Lambert, Jani Särkkä, and Pauli Virtanen for fruitful collaboration. In addition, I appreciate the valuable discussions with Manuel Houzet, Andrzej Kolek, Mikko Kärkkäinen, Pritiraj Mohanty, Juha-Matti Perkkiö, Fabio Pistolesi, and Mika Silanpää.

A substantial part of the funding of this work has been granted by the Finnish Cultural Foundation, the Magnus Ehrnrooth Foundation, the Foundation of Technology (TES, Finland), and Antti and Jenny Wihuri Foundation through personal scholarships, all of which institutions I gratefully acknowledge. The computing resources have been provided by the Center for Scientific Computing (CSC).

In autumn 2005 the Theory Group of the Materials Physics Laboratory was combined with Dr. Ari Harju's research group in the Laboratory of Physics. In what I think turned out to be a successful merger, the Quantum Many-Body Physics Group was formed. I would like to thank Ari and all the members of the Group as well as the other personnel in the Laboratory of Physics for a pleasant working atmosphere. Furthermore, I recall the fun and enlightening discussions with several people in different conferences and summer schools. Likewise, I am grateful to my friends for the joyous moments spent both in academic and extracurricular activities.

Moreover, I thank my relatives for interest in my pursuits.

Finally, I am indebted to Krista for support and introducing me to various other aspects of life.

Espoo, May 2007

Markku Stenberg

Contents

Affiliation	vii
Preface	ix
Contents	xi
List of Publications	xiii
Author’s contribution	xiv
1 Introduction	1
2 Quantum coherent transport phenomena	7
2.1 Superconductivity and supercurrent	7
2.2 Andreev reflection and superconducting proximity effect	9
2.3 Reentrance effect	10
2.4 Reflectionless tunneling	11
2.5 Localization and fluctuations	13
2.6 Correlations of the charge transfers	14
2.7 Conductance and current cumulants	15
3 Nambu-Keldysh formalism	17
3.1 Bogoliubov-de Gennes equations	17
3.2 Quasiclassical Keldysh Green’s function formalism	18
3.2.1 Full counting statistics	25
3.2.2 Noise correlations	27
4 Random matrix theory	30
4.1 Scattering theory	30
4.2 Dorokhov-Mello-Pereyra-Kumar equation	31
5 Scattering approach to quantum transport	36

6 Discussion	38
References	42

List of Publications

This Thesis consists of an overview and of the following publications which are referred to in the text by their Roman numerals.

- I** Markku P. V. Stenberg and Jani Särkkä, *Higher-order mesoscopic fluctuations in quantum wires: Conductance and current cumulants*, Phys. Rev. B **74**, 035327 (2006).
- II** Markku P. V. Stenberg, Pauli Virtanen, and Tero T. Heikkilä, *Phase-dependent noise correlations in normal-superconducting structures*, Helsinki University of Technology, Publications in Engineering Physics A, Report TKK-F-A852 (2007) (submitted for publication).
- III** Markku P. V. Stenberg and Tero T. Heikkilä, *Nonlinear shot noise in mesoscopic diffusive normal-superconducting systems*, Phys. Rev. B **66**, 144504 (2002).
- IV** Tero T. Heikkilä, Markku P. Stenberg, Martti M. Salomaa, and Colin Lambert, *Thermopower in mesoscopic normal-superconducting structures*, Physica B **284-8**, 1862 (2000).
- V** Ari T. Alastalo, Markku P. V. Stenberg, and Martti M. Salomaa, *Response functions of an artificial Anderson atom in the atomic limit*, J. Low Temp. Phys. **134**, 897 (2004).

Author's contribution

The work reported in this Thesis has been carried out in the Theory Group of the Materials Physics Laboratory and in the Quantum Many-Body Physics Group of the Laboratory of Physics at the Helsinki University of Technology.

The author has extensively contributed to the research reported in this Thesis. The analytical calculations for Paper II and to a substantial degree for Paper I have been conducted by him. An essential part of the computer codes used in Papers II, III and IV have been developed by him. He has carried out the numerical calculations in Papers II and III and participated in the analysis of the results of Papers IV and V. The Figures in Papers II and III were produced by him.

Papers I, II, III, and partially Paper V were written by him. The author has presented the research findings of this Thesis at several international conferences and workshops.

1 Introduction

Physical systems cold and small enough may exhibit certain distinctive quantum features. First, because of the wave nature of matter, the alternative paths for its time evolution influence simultaneously the outcome of the measurement. For example, an electron may interfere with itself [1–3]. Second, it may be necessary to know the behavior of an object as a whole instead of the sum of its parts. The many-body correlation effects that may affect the behavior of the electric current [4–6] provide one example. Third, a large numbers of particles may collectively behave like a single quantum state. For instance, when a piece of metal has turned into a superconducting state, its conduction electrons share a definite quantum mechanical phase [7–10]. These phenomena constitute examples of the features characteristic for systems referred as coherent.

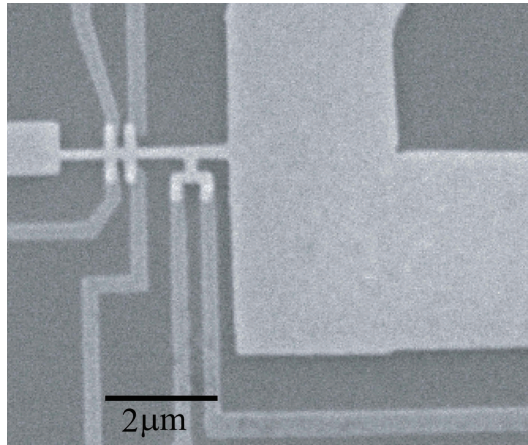


Figure 1.1: Scanning electron microscope image of a normal-superconducting nanostructure. The bright areas are patterned from a silver film (a normal metal). The slightly darker wires are made of aluminum (a superconductor below its critical temperature T_c). The types of thermoelectric effects studied in Paper IV can be measured in this kind of structures. In a bulk metal, T_c for aluminum is 1.1 K ; in a film, T_c is somewhat higher. (Courtesy of Igor Sosnin, the scale bar added by the author.)

At the borderline of the microscopic and macroscopic world resides a regime which is called mesoscopic. Mesoscopic systems are small enough to exhibit quantum

coherent behavior, yet they contain a sufficiently large number of particles to allow a statistical description, e.g., through distribution functions. Mesoscopic conductors [11–13] (Fig. 1.1) may be considered as a realistic platform for future nanoelectronics since they should allow for scalability and integration. Such mesoscopic circuits might deliver new applications, such as quantum computing. Making use of novel device architectures, e.g., superconducting transistors or quantum bits, they might also outperform conventional electronics due to higher current densities, lower power consumption and faster switching times.

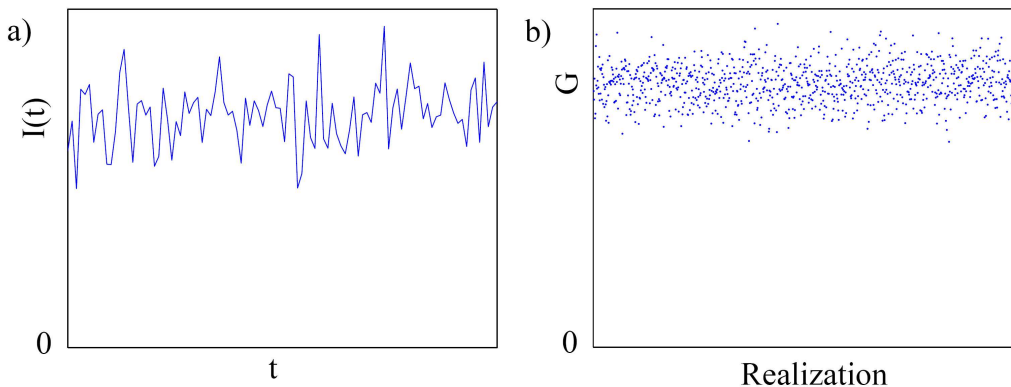


Figure 1.2: The current transferred through a mesoscopic conductor varies in time (a). The width of the current distribution in Fig. 1.2a is $\sqrt{S_I/t_0}$, with the noise power S_I and measurement time t_0 . In an ensemble of disordered conductors, the conductances vary from sample to sample (b). The width of the conductance distribution in Fig. 1.2b is $\sqrt{\text{Var } G}$.

In all electronic conductors, the flow of electric current exhibits statistical fluctuations. In macroscopic conductors, the noise in the flow of particles mostly arises from the dominant thermal fluctuations. However, even at vanishing temperature, the charge transferred through a mesoscopic sample in unit time varies due to the quantum, i.e., discrete and probabilistic, nature of the transport process (Fig. 1.2a). Further, also the time-averaged quantities change if the configuration of disorder which scatters the particles in the structure is altered, e.g., through annealing the sample for a short time [14] (Fig. 1.2b). These variations are called mesoscopic fluctuations.

tuations. Mesoscopic fluctuations provide information on the physics of transport phenomenon not contained in conductance, e.g., on the unit charge of the elementary excitations and on the correlations between charge transfers.

In a metal, conduction electrons scatter from impurities and imperfections of the underlying ionic lattice such that usually the mean free path l_{el} , the length scale over which the electrons lose their memory¹ on the direction of their initial velocity, is of the order of 1 – 100 nm. However, elastic scatterings from nonmagnetic or static impurities do not destroy the fixed phase relationship of electrons [15]². Hence, at low temperatures, the phase coherence length λ_{φ} , i.e., the distance over which the phase of an electron remains correlated to its initial value, may vastly exceed l_{el} . Since the end of 1980s, experiments at sub-Kelvin temperatures have been performed with λ_{φ} of the order of micrometers [18–21], and in recent measurements [22–24], λ_{φ} of the order of one hundred micrometers has been achieved.

Transport experiments may also yield more specific information about the phase coherence of the electrons. The types of transport experiments mentioned here may be conducted [25], for example, by the use of the structures consisting of wires or loops made of normal (e.g., Au, Pd, Ag or Cu) or superconducting (e.g., Al, Pb, Sn or Nb) metals, in carbon structures [26, 27], or in a two-dimensional electron gas formed at an interface between two different semiconductors (e.g., AlGaAs and GaAs). For example the standard procedure to determine λ_{φ} is to fit the prediction of the theory for the quantum interference effect of weak localization [28] to magnetoresistance measurements. In the past few years, advances on the measurements [29–34] of higher-order mesoscopic fluctuations have also been made, and presently experiments up to the sixth current cumulant and fourth conductance cumulant have been performed. In normal-metal structures the nature of transport is typically diffusive but, e.g., in graphene, carbon nanotubes, or two-dimensional electron gas at a semiconductor interface, electrons can travel over the length scales

¹The time evolution of particles is invertible but this statement has to be understood in a more macroscopic sense. That is, if the exact impurity configuration is unknown, the information about the initial quantum state vanishes on a time scale $\tau_{\text{el}} = l_{\text{el}}/v_F$, with v_F the magnitude of the Fermi velocity.

²The energy exchange between a system and its environment is not necessary for dephasing nor do inelastic processes always destroy phase coherence [16, 17].

of the order of micrometers without being scattered. In these condensed matter systems, the major sources for dephasing are usually electron-electron, electron-phonon and magnetic impurity interactions [35].

There are several reasons to investigate mesoscopic fluctuations in phase coherent systems. First, studying fluctuations is a way to extend the existing theories for the fluctuation point of view, for example, for the superconducting proximity effect, reflectionless tunneling, or weak localization. This is one of the goals of this Thesis. As an example, the superconducting proximity effect induces sort of "superconducting" properties in a normal metal. Until the beginning of this decade, the studies of the superconducting proximity effect concentrated on the influence of the effect on electric conductance. Since the discovery of the phenomenon it has been known that due to the superconducting proximity effect correlations between electrons and holes in a normal-metal arise. Studying shot noise (Papers II and III) reveals that, in addition, the superconducting proximity effect induces anticorrelations between different electron-hole pairs in a normal metal.

A second motivation for the study of mesoscopic fluctuations is the fact that they can be used as a test bench for conventional condensed matter theories. For example, the one-parameter scaling model [36] is a kind of cornerstone of mesoscopic physics. In Subs. 2.7 we introduce the conductance and current distributions characterizing mesoscopic fluctuations and define conductance and current cumulants. The one-parameter scaling hypothesis suggests that the dimensionless conductance $g \equiv hG/e^2$ is the only relevant parameter that governs the evolution of conductance distribution with sample size L . A well-known consequence of the noninteracting scaling model is that for the n th conductance cumulant, say, in the absence of time reversal symmetry, one has $\langle\langle g^n \rangle\rangle \sim \langle g \rangle^{2-n}$ (see, e.g., Ref. [37]). Or so it was thought. In Paper I we prove by a detailed calculation that the correct result for the conductance cumulants higher than second is actually $\langle\langle g^n \rangle\rangle \sim \langle g \rangle^{-n}$. Both expressions, however, yield small values for these higher-order cumulants. But in the experiments [29], where the third and fourth conductance cumulants in metallic wires were measured, considerably larger values were observed under certain conditions. If correct, these results of the measurements would constitute a violation of

the one-parameter scaling model. A noninteracting model may also bear relevance in the studies of interactions. Mohanty and Webb, the authors of Ref. [29], suggest that the failure of the scaling model in these experiments would be caused by the electron-electron interactions but these conclusions have not been accepted without skepticism (see Refs. [38, 39]) and the situation has remained somewhat unclear. Besides these measurements of higher-order conductance cumulants, in another experiment, inconsistencies were found when λ_φ was inferred from two independent methods: through weak-localization measurements and the measurements of the time-dependent universal conductance fluctuations [40].

A third aspect in the study of fluctuations is more technologically oriented. For example, multiterminal structures carrying supercurrent through a normal-metal weak link have been suggested for a realization of a superconducting transistor [41], and have been used for quantum-bit measurements [42]. Quantum information may be encoded in the direction of the supercurrent which can be controlled by tuning the electrostatic potential of a normal-metal terminal [43, 44]. Recently, the nonequilibrium current noise in such superconducting transistors has been investigated (see, e.g., Paper II). In some cases the current fluctuations might find application relevance, such as, shot noise which can be used to measure the properties of normal-superconducting interfaces as we discuss in Subs. 2.4 and Paper III.

Outline of the Thesis

This Thesis presents the author’s work on the theory of quantum coherent mesoscopic systems with the emphasis on mesoscopic fluctuations. The overview serves as an introduction to Papers I–V that contain the author’s contributions to the topic. Section II describes, on a qualitative level, some of the quantum coherent effects studied in this dissertation. The treatment of Sec. II should be accessible also for nonspecialists. In the Secs. III–V, a short introduction, from a perspective determined by the focus of this Thesis, to the quasiclassical Nambu-Keldysh formalism, the random matrix theory, and the scattering approach to quantum transport is given. The presentation in Secs. III–V is targeted for a reader who wishes to follow the calculations in more detail. Section VI summarizes the results and discusses

some open problems and the development of the field.

2 Quantum coherent transport phenomena

2.1 Superconductivity and supercurrent

Many metals, such as aluminum, lead, tin or niobium, can carry electric current without dissipation, supercurrent, below certain material specific critical temperature T_c . For conventional superconductors T_c ranges from less than 1 K to around 20 K [10, 45]. Below T_c , correlated pairs of the conduction electrons, Cooper pairs, are formed. In conventional superconductors, the Cooper pairing is brought forth by an attractive interaction, with coupling strength λ , which is mediated by phonons. The average distance of the conduction electrons is of the order of Fermi wavelength or $\mathcal{O}(0.1 \text{ nm})$ [45]. The characteristic length, the superconducting coherence length ξ_S , over which the correlations, described by the pairing amplitude F , of the quasiparticles extend, is much larger, typically of the order of $\mathcal{O}(10 - 100 \text{ nm})$ [46]. Further, the global gauge symmetry is broken and the quantum mechanical phase of the electron system becomes "rigid" [47]. Hence a pairing potential $\Delta = |\Delta|e^{i\phi} = \lambda F$, which essentially describes a macroscopic wave function, may be introduced [7–10]. In a normal metal, the state of an electron may be changed by adding an arbitrarily small amount of energy but there is a minimum amount of energy, $|\Delta| \sim T_c$, that must be supplied in order to break apart or excite the electrons bound into Cooper pairs³. By coherent tunneling of Cooper pairs, supercurrent also flows through a thin insulating barrier, a so-called weak link, between two superconductors provided there is a finite phase difference between the superconductors [48]. Through a different mechanism, a weak link composed of a wider piece of a normal metal or semiconductor may also carry supercurrent [49]. In a two-terminal setup, the supercurrent can basically be controlled only by the phase difference between the superconductors and the external temperature, but in multi-terminal devices it is possible, and also experimentally feasible [43, 44], to invert the direction of supercurrent by an external control voltage. This may be achieved by applying the control voltage V in a normal terminal connected to a weak link and tuning the microscopic current-carrying elec-

³Natural units with $\hbar = k_B = 1$ are used throughout the Thesis unless otherwise indicated.

tronic states through V [41,50,51]. A possible setup is illustrated in Fig. 2.1, where the supercurrent I flows between the superconducting terminals T_1 and T_2 and V is applied to the normal terminal T_3 . This kind of structure is particularly relevant for information processing since it is suitable for a realization of a superconducting transistor. In Paper II we studied current noise in such nanostructures. Unlike a

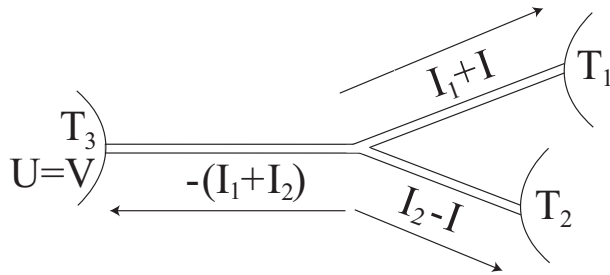


Figure 2.1: Setup schematic of a three-terminal nanostructure.

dissipative current, supercurrent also flows when the system is in equilibrium, without any applied voltage. Since it is a ground state property of the system, one may anticipate that supercurrent does not fluctuate⁴. Neither does supercurrent induce its own correlations in the current fluctuations in the presence of dissipative currents. Consider, e.g., the three-terminal setup in Fig. 2.1, consisting of diffusive wires. As long as only normal currents are concerned, the correlations of current fluctuations in, say, terminals 2 and 3, measured by covariances of incoming charges, depend on the direction of the current I . However, if the current I is supercurrent, these covariances are not altered upon the reversal of I . This means that the dissipative current is in no way correlated with the supercurrent. However, the presence of the latter changes the correlations of the charge transfers, and the $I - V$ curve, in the previous (see Paper II).

⁴Under certain conditions coherent multiple Andreev reflections may change this picture, see, e.g., Ref. [52].

2.2 Andreev reflection and superconducting proximity effect

In the first quantization picture, the scattering processes at the normal-superconducting interface may be viewed by studying the quasielectrons and holes reflected at the boundary. A quasielectron incident from the normal metal with an energy below the gap $|\Delta|$ can not enter the superconductor but is reflected back as a hole which carries information about the phase of the incident particle and the superconducting condensate, cf., Fig. 2.2a. This is called Andreev reflection [10, 53, 54]. In the process an additional electron is removed from the normal side and a Cooper pair is formed in the superconductor. Close to the Fermi surface, the reflected hole has a velocity with equal magnitude but opposite direction as the incident electron. Immediately after the Andreev reflection the electron-hole pair is coherent. Hence close to the Fermi surface, the reflected hole-like wave takes the same path as the incident particle-like wave but in the opposite direction. With larger energies, however, the electron-hole pair dephases. The picked-up phase difference is proportional to the wave vector mismatch and the distance travelled from the interface $\delta\varphi = 2 \int dx \cdot \delta\mathbf{k}$ (Fig. 2.2b). In the opposite process, an incident hole may reflect as an electron such that a Cooper pair is removed from the superconductor.

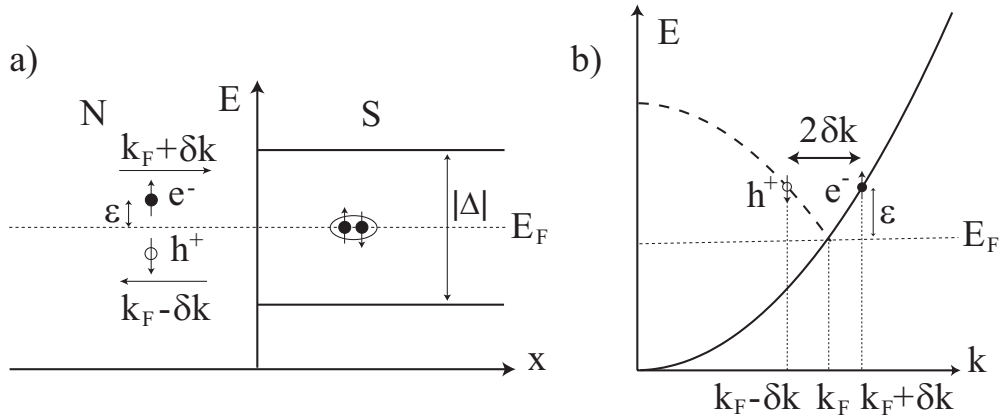


Figure 2.2: Schematic illustration of the Andreev reflection at an NS interface in real (a) and momentum (b) space. The dephasing rate of electrons and holes is proportional to the wave vector mismatch δk .

In a piece of a normal metal (N) in good contact to a superconductor (S) the local density of states and transport properties near the interface are modified [55]. The electron-hole pairs, called Andreev pairs, remain correlated in the normal metal since F is a smooth function across the interface (Fig. 2.3). This is called the super-

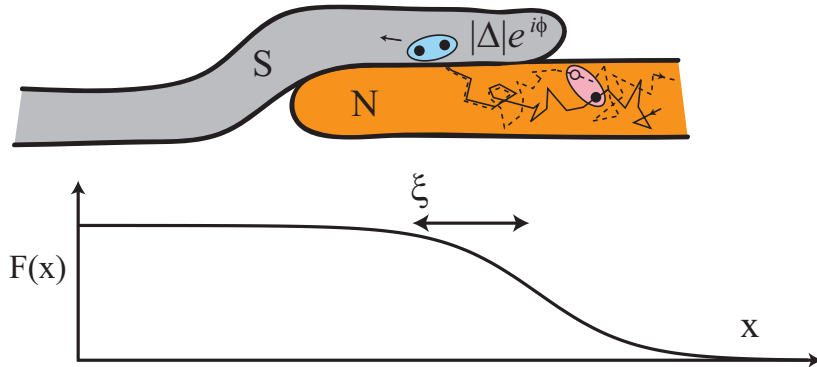


Figure 2.3: Superconducting proximity effect in a typical normal-superconductor contact, an overlap junction. In a normal metal, the superconducting pairing amplitude decays on a length scale ξ . The Andreev reflected particle carries information about the phase of the incident particle and the superconducting condensate.

conducting proximity effect. However, there is no attractive interaction between the electrons on the normal side. Consequently F decays exponentially on the length scale ξ_N . In the case of diffusive transport, $\xi_N = \sqrt{D/\varepsilon^*}$, with D the diffusion constant, may be hundreds of nanometers at low temperatures. Here ε^* is the largest relevant energy scale, which may be, e.g., T , or, in nonequilibrium, eV .

2.3 Reentrance effect

How does the proximity effect affect the transport characteristics of a normal metal? Let us consider a diffusive wire between N and S terminals (Fig. 2.4). The effective charge carrying unit is a Cooper pair with charge $2e$. The characteristic energy scale or the width of the energy levels of the system, Thouless energy $E_T = D/L^2$, is inversely proportional to the time it takes for a particle to diffuse across the sample

of length L and with diffusion constant D .

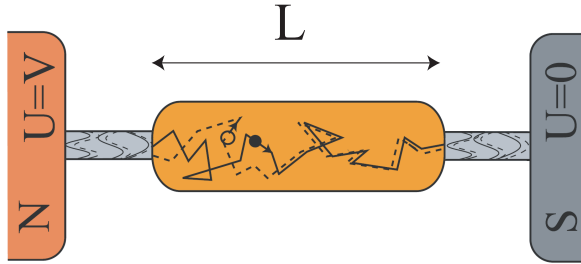


Figure 2.4: Long NS junction composed of normal and superconducting terminals and a diffusive normal-metal wire. The superconducting proximity effect affects the transport properties of the system when electrons and holes dephase on a length scale comparable to the sample size, i.e., $L \sim \xi = \sqrt{D/\varepsilon}$.

When the transport is fully phase coherent, i.e., at low voltages, the Andreev-reflected partial waves trace back the trajectory of the initial waves. Even though the effective charge in the transport process is twice that of a single electron, conductance is not altered, since the effective length in the process is also doubled [56]. The trajectory related to the transfer of charge $2e$ is composed of the paths of the initial and reflected particles.

Also in the case where electrons and holes dephase on a length scale much smaller than the wire length, and their motion is totally uncorrelated, i.e., at high voltages, conductance exhibits its normal-state value. When, however, the electrons and holes dephase at the length scale comparable to the wire length, i.e., at the voltages of the order of E_T/e , their correlations alter the transport characteristics. The differential conductance exhibits a maximum at about $eV = 5E_T$ and a similar, but not identical, effect is observed in the differential shot noise (cf., Papers II and III).

2.4 Reflectionless tunneling

In electric circuits, an insulating barrier can be formed at the interface of two metals, e.g., by oxidation. Consider a normal and superconducting metal separated by such a barrier and quasielectrons and holes incident from the normal side and undergoing normal and Andreev reflections at the interface. A particle-like wave which hits the

barrier is partially retroreflected back as a hole and partially reflected as a particle-like wave which may again hit the barrier having scattered in the diffusive metal (see Fig. 2.5). Near the Fermi surface, the quasiparticles (holes) and the Andreev-reflected holes (quasiparticles) move along the same paths in opposite directions. On the trajectories which begin and end at the barrier, the particle and hole-like waves constructively interfere which increases the number of "attempts" for transmission. If the material on the normal-metal side is disordered enough, many scatterings between the diffusive metal and the tunneling barrier take place, and conductance through the barrier is increased [57, 58]. Ideally, the conductance at low voltages equals that of a transparent contact. Hence the phenomenon is called reflectionless tunneling. At larger energies, where the paths of the quasiparticles and retroreflected holes do not coincide, the effect is suppressed. In paper III we showed that also shot noise is increased by reflectionless tunneling. Since the effective charge characterizing shot noise is a function of the barrier height, shot noise may be used to measure the strength of the insulating barrier.

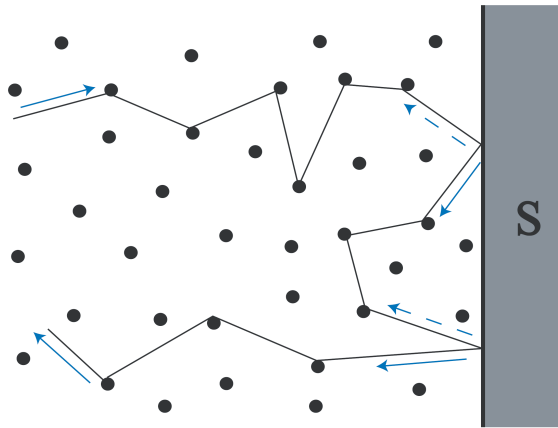


Figure 2.5: Illustration of the reflectionless tunneling effect. On the trajectories which begin and end at the barrier at the NS interface, the particle and hole-like waves constructively interfere. This modifies the transport characteristics at low voltages.

2.5 Localization and fluctuations

In a disordered medium, the direction of motion of quasiparticles is randomized due to scatterings on a length scale l_{el} . Weak localization and weak antilocalization result from the interference of the closed trajectories of the electron and their time-reversed counterparts (Fig. 2.6). In a phase coherent conductor, in the presence

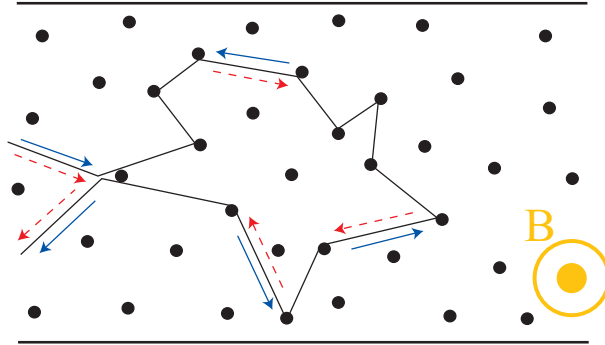


Figure 2.6: Illustration of the weak (anti)localization effect. The interference between the partial waves on a closed trajectory and its time-reversed counterpart may increase or decrease the coherent backscattering probability. The magnetic field B suppresses the effects.

of time-reversal and spin-rotation symmetries, the amplitude of a closed Feynman path equals that of the time-reversed path. In the case of broken spin rotation symmetry, however, the spins of the partial waves are rotated in negatively correlated directions⁵. Consequently, destructive interference of the closed paths may be realized in a material with strong spin-orbit interaction, or through the Elliot-Yafet mechanism [59]. Strong spin-orbit scattering is observed, e.g., in samples made of gold [60, 61]. The resulting enhanced (reduced) backscattering reduces (enhances) conductance, and is called weak (anti)localization. A magnetic field breaks time-reversal invariance and suppresses these effects. Putting all together, in a normal-metal conductance is modified by a term proportional to $(m_0 - 2)/m_0$, where m_0 may obtain the value 1, 2 or 4, and describes the symmetries in the system [62–64] (cf., Sec. 4 and standard classes in Table 4.1).

⁵The statistical expectation value of the inner product between a normalized spin state and its time-reversed counterpart equals $-1/2$.

If the disorder configuration of a mesoscopic sample is altered, e.g., through annealing, its conductance changes. These conductance fluctuations have a universal magnitude with the variance $\text{Var } G = 4e^2/(15hm_0)$ [62–64]. An ensemble of "disorder realizations" may also be generated by sweeping the magnetic field [65] or changing the gate-voltage [66] in the setup. This phenomenon, referred as universal conductance fluctuations, is also due to the interference of the partial waves of an electron.

The conductance of an incoherent wire is inversely proportional to the length L of the wire according to Ohm's law, but in a phase coherent wire quantum interference may change the situation drastically. If L is larger than the Anderson localization length λ_{loc} ,⁶ i.e., the scale on which the nature of the electronic states is localized instead of spatially extended, the transmission eigenvalues are close to zero and conductance decreases exponentially as a function of L [67]. This is referred as strong localization. In the metallic region, the Ohm's law is valid fairly well but corrections, e.g., due to weak localization arise. The transmission eigenvalues are not evenly distributed in this case either, but the corresponding distribution has a bimodal shape [68, 69]. The region where the transmission eigenvalues are close to unity, with L comparable to l_{el} , is called ballistic.

2.6 Correlations of the charge transfers

Consider elementary excitations with charge q traversing through a mesoscopic sample and crossing a counter at a terminal at random times $\{t_i\}$. In the static case the average current is $\bar{I} = \langle q \sum_i \delta(t - t_i) \rangle$. The zero-frequency noise power, i.e., shot noise, describes correlations of current at different times t and t' . Shot noise reads

$$\begin{aligned}
 S &= 2 \int_{-\infty}^{\infty} d(t - t') \langle \hat{I}(t) \hat{I}(t') - \bar{I}^2 \rangle = 2 \int_{-\infty}^{\infty} d(t - t') \left\langle q^2 \sum_{ij} \delta(t - t_i) \delta(t' - t_j) - \bar{I}^2 \right\rangle \\
 &= 2q\bar{I} + 2 \int_{-\infty}^{\infty} d(t - t') \left\langle q^2 \sum_{i \neq j} \delta(t - t_i) \delta(t' - t_j) - \bar{I}^2 \right\rangle.
 \end{aligned} \tag{2.1}$$

Thus the shot noise yields information on the effective charge carrying unit q in the transport process. Generally, the correlation of two separate statistical variables A_i

⁶In a quasi-one dimensional conductor the localization length is given by $\lambda_{\text{loc}} = N_c l_{\text{el}}$.

and A_j (with $i \neq j$) is measured by $\langle A_i A_j - \bar{A}_i \bar{A}_j \rangle$. In Eq. (2.1), the second term on the second line describes the correlations between separate transport events. It vanishes when the different processes are uncorrelated and is negative in the presence of anticorrelations. In a tunnel junction or a vacuum diode, transport processes are uncorrelated and the shot noise is given by the Schottky formula $S = 2e\bar{I}$ [70]. In an NS junction, in the absence of the superconducting proximity effect, shot noise, $S = 4e\bar{I}$, as well as the effective charge (cf. Subs. 2.2) is doubled.

Except for the tunneling limit, Fermi statistics reduce shot noise below the Schottky value. In terms of the transmission eigenvalues $\{T_i\}$, the differential shot noise is given by $dS/dV = (4e^2/h) \sum_i T_i(1 - T_i)$, as long as energy is conserved in the transport process. Due to the Pauli principle, open ($T_i = 1$) or closed ($T_i = 0$) transmission channels do not fluctuate or contribute to the shot noise. In a diffusive normal-metal wire, where the transmission eigenvalue density takes a bimodal form (cf., Subs. 2.5, Fig. 4.2), shot noise has a universal value $S = (2e/3)\bar{I}$ [71]. In a long NS junction (Fig. 2.4), at low and high voltages where the superconducting proximity effect is negligible, shot noise is given by $S = (4e/3)\bar{I}$. At voltages of the order of E_T/e , besides correlations between electrons and holes, superconducting proximity effect induces anticorrelations between Andreev pairs, which suppresses shot noise. In Paper II we found that the low-voltage behavior of shot noise is a result of a competition between anticorrelation of Andreev pairs and the depression of the local density of states.

2.7 Conductance and current cumulants

The types of fluctuation and localization phenomena discussed in Sec. 1 and Subs. 2.5, 2.6 may be conveniently studied by the distributions of two dimensionless variables: N , the number of particles transmitted through a sample in unit time and $g = hG/e^2$, a dimensionless conductance. The probability distribution $P(x)$ of a statistical variable x may be characterized by the generating function $f(y)$ and

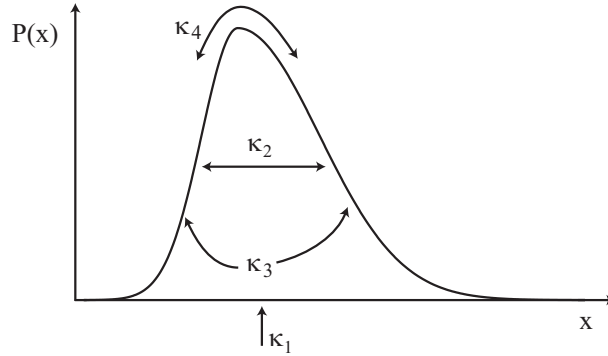


Figure 2.7: Illustration of the cumulants κ_1 (average), κ_2 (width), κ_3 ("skewness") and κ_4 ("sharpness") of a probability distribution.

cumulants κ_n

$$f(y) \equiv \ln \langle e^{yx} \rangle = \ln \left(\sum_x P(x) e^{yx} \right) = \ln \left(\int dx P(x) e^{yx} \right), \quad \kappa_n \equiv \frac{\partial^n}{\partial y^n} f(y) \Big|_{y=0}. \quad (2.2)$$

In the first equation, the third and fourth expression apply for a discrete and continuous variable x , respectively. These definitions imply that the first and second cumulants are the mean and variance of $P(x)$, respectively, while the higher cumulants measure the deviation of $P(x)$ from the Gaussian form (Fig. 2.7)

$$\kappa_1 = \langle x \rangle, \quad \kappa_2 = \langle (x - \langle x \rangle)^2 \rangle, \quad \kappa_3 = \langle (x - \langle x \rangle)^3 \rangle, \quad \kappa_4 = \langle (x - \langle x \rangle)^4 \rangle - 3 \langle (x - \langle x \rangle)^2 \rangle^2. \quad (2.3)$$

Current cumulants C_n are obtained by making in Eqs. (2.2), (2.3) the substitutions

$$x \rightarrow N, \quad P(x) \rightarrow P_{t_0}(N), \quad \kappa_n \rightarrow C_n, \quad (2.4)$$

with $P_{t_0}(N)$ the probability of N particles being transmitted through a sample in time t_0 . For conductance cumulants, the notations

$$x \rightarrow g, \quad P(x) \rightarrow P(g), \quad \kappa_n \rightarrow \langle\langle g^n \rangle\rangle \quad (2.5)$$

are usually adopted. In Paper I the six lowest conductance cumulants and the ten lowest current cumulants for a quasi-one-dimensional wire in the metallic region were calculated.

3 Nambu-Keldysh formalism

This Section gives a brief introduction to quasiclassical Keldysh Green’s function formalism. This method has become the standard approach to study nonequilibrium quantum transport in diffusive normal-superconducting nanostructures but it can not account for such interference effects as the localization behavior of electronic states or conductance fluctuations. The equation governing the transport statistics in such systems is the Usadel equation [see Eq. (3.10)] for a generalized quasiclassical Green’s function. In principle, it is possible to describe the transport characteristics of a given system by a method based on a direct discretization of the Usadel equation. For noise (or higher current cumulants), such calculations, however, become computationally heavy and do not provide much interpretation for results. A physically more transparent and computationally more efficient approach is to parametrize the equations and look for the solutions for these parameters. For conductance, in the presence of the superconducting proximity effect, such parametrizations have been used since the 1990s [72]. In the absence of supercurrent, a parametrization to calculate shot noise was recently found [73]. In Paper II we give a parametrization, applicable also in the presence of supercurrent, to calculate noise correlations.

3.1 Bogoliubov-de Gennes equations

At low temperatures and excitation energies, the conduction electrons of a normal metal may be described by substituting the non-interacting fermions with elementary excitations or quasiparticles, each of which carries the same quantum numbers as the original particles. The quasiparticles may be thought of as particles who perturb the motion of the particles in their vicinity and are ”screened” by the positive charge of the background ions. Such Fermi systems, which, in many respects, are analogous to a Fermi gas, are called Fermi liquids [74–76].

In the presence of attractive interactions this picture has to be modified. The excitations in the heterostructures consisting of normal metals and spin-singlet su-

perconductors may be described by the effective one-electron Hamiltonian

$$H_{\text{eff}} = \int d\mathbf{r} \sum_{\alpha} \left(\hat{\psi}_{\alpha}^{\dagger}(\mathbf{r}) H_0 \hat{\psi}_{\alpha}(\mathbf{r}) + \hat{\psi}_{\alpha}^{\dagger}(\mathbf{r}) U(\mathbf{r}) \hat{\psi}_{\alpha}(\mathbf{r}) \right) + \Delta(\mathbf{r}) \hat{\psi}_{\uparrow}^{\dagger}(\mathbf{r}) \hat{\psi}_{\downarrow}^{\dagger}(\mathbf{r}) + \Delta^*(\mathbf{r}) \hat{\psi}_{\downarrow}(\mathbf{r}) \hat{\psi}_{\uparrow}(\mathbf{r}), \quad (3.1)$$

with $H_0 \equiv -\nabla^2/2m - E_F$, and the pairing potential $\Delta(\mathbf{r}) \equiv \lambda(\mathbf{r}) \langle \hat{\psi}_{\uparrow}(\mathbf{r}) \hat{\psi}_{\downarrow}(\mathbf{r}) \rangle$. The real-space field operator in Schrödinger picture with spin α is denoted by $\hat{\psi}_{\alpha}(\mathbf{r})$ and $\lambda(\mathbf{r})$ is the coupling strength. The Hamiltonian H_{eff} may be diagonalized by the canonical Bogoliubov transformation

$$\hat{\Psi}(\mathbf{r}) \equiv \begin{pmatrix} \hat{\psi}_{\uparrow}(\mathbf{r}) \\ \hat{\psi}_{\downarrow}^{\dagger}(\mathbf{r}) \end{pmatrix} = \sum_{n>0} \left[\hat{\gamma}_{n\uparrow} \begin{pmatrix} u_n(\mathbf{r}) \\ v_n(\mathbf{r}) \end{pmatrix} - \hat{\gamma}_{n\downarrow}^{\dagger} \begin{pmatrix} v_n^*(\mathbf{r}) \\ -u_n^*(\mathbf{r}) \end{pmatrix} \right]. \quad (3.2)$$

Here $\hat{\Psi}(\mathbf{r})$ is a vector in Nambu, i.e., electron-hole space [77], and $\hat{\gamma}_{n\uparrow}, \hat{\gamma}_{n\downarrow}^{\dagger}$ are destruction and creation operators for quasiparticles. The amplitudes $u_n(\mathbf{r})$ and $v_n(\mathbf{r})$ obey the Bogoliubov-de Gennes equations [7]

$$\begin{pmatrix} H_0 + U(\mathbf{r}) & \Delta(\mathbf{r}) \\ \Delta^*(\mathbf{r}) & -[H_0 + U(\mathbf{r})] \end{pmatrix} \begin{pmatrix} u_n(\mathbf{r}) \\ v_n(\mathbf{r}) \end{pmatrix} = \varepsilon_n \begin{pmatrix} u_n(\mathbf{r}) \\ v_n(\mathbf{r}) \end{pmatrix}, \quad (3.3)$$

which constitute a self-consistent set of equations where the pairing potential is obtained from $\Delta(\mathbf{r}) = \lambda(\mathbf{r}) \sum_{n>0} v_n^*(\mathbf{r}) u_n(\mathbf{r}) [1 - 2f(\varepsilon_n)]$. Here ε_n are excitation energies. For each positive energy solution $(u_n(\mathbf{r}), v_n(\mathbf{r}))^T$ of Eq. (3.3) there exists a solution $(v_n^*(\mathbf{r}), -u_n^*(\mathbf{r}))^T$ with negative energy $-\varepsilon_n$. At the normal-superconducting interface, $\lambda(\mathbf{r})$ diminishes to zero at the length scale of the Fermi wavelength. In practical calculations, the attractive interaction is usually assumed to vanish in the normal-metal and set to some finite constant in a superconductor.

3.2 Quasiclassical Keldysh Green's function formalism

Imagine the time coordinate running from t_i to t_f along the curve c_1 and back along c_2 as in Fig. 3.1. This curve, c_K , is called the Keldysh contour. The Keldysh formalism [35, 54, 78, 79] is convenient for the study of systems out of equilibrium, but also for equilibrium systems it provides a natural theoretical framework. There are four ways to place two time coordinates t and t' on the two parts, c_1 and c_2 , of

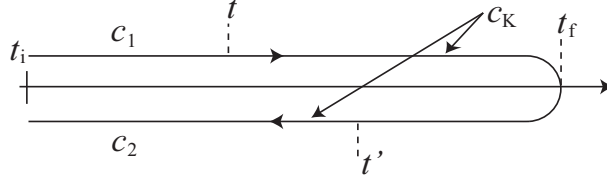


Figure 3.1: The Keldysh contour c_K . There are four ways to place two time coordinates t and t' on the two parts, c_1 and c_2 , of c_K . The ordering corresponding to the upper-right element of the matrix (3.4) is illustrated in Figure.

the time contour. Hence the Green's function time ordered with respect to contour c_K may be represented by introducing the following matrix structure

$$\check{G}_{\text{ur}}(1, 1') = \begin{pmatrix} -i\langle \overrightarrow{T} \hat{\psi}(1) \hat{\psi}^\dagger(1') \rangle & i\langle \hat{\psi}^\dagger(1') \hat{\psi}(1) \rangle \\ i\langle \hat{\psi}(1) \hat{\psi}^\dagger(1') \rangle & i\langle \overleftarrow{T} \hat{\psi}(1) \hat{\psi}^\dagger(1') \rangle \end{pmatrix}. \quad (3.4)$$

Here the field operators are represented in the Heisenberg picture. In their arguments, a compact notation has been introduced such that $1 \equiv (\mathbf{r}_1, t_1)$ etc. The time-ordering and anti-timeordering operators are denoted by \overrightarrow{T} and \overleftarrow{T} , respectively. The expectation value $\langle \dots \rangle$ is taken over the quantum state of the system. In the Green's function the subscript ur refers to 'unrotated'. All the elements of \check{G}_{ur} are not independent but one of the submatrices may be eliminated by performing the Keldysh rotation⁷

$$\check{L} \check{G}_{\text{ur}} \check{L}^\dagger(1, 1') = \begin{pmatrix} \hat{G}^R(1, 1') & \hat{G}^K(1, 1') \\ \hat{0} & \hat{G}^A(1, 1') \end{pmatrix} \equiv \check{G}_{\text{rot}}(1, 1'), \quad \check{L} = \hat{\tau}_0 \otimes (\bar{\sigma}_0 - i\bar{\sigma}_2) / \sqrt{2}. \quad (3.5)$$

This equation may be taken as a definition for the retarded, advanced and Keldysh Green's functions, $\hat{G}^A, \hat{G}^R, \hat{G}^K$. Here $\hat{\tau}_i, \bar{\sigma}_j$ are matrices in Nambu ($\hat{\cdot}$) and Keldysh ($\check{\cdot}$) space. The spectral or equilibrium properties are described by \hat{G}^R and \hat{G}^A , whereas \hat{G}^K contains information about the (nonequilibrium) distributions of the electrons and holes. In the following, the subscripts for \check{G} are dropped since the derivations of the equations of motion do not depend on the representation of the

⁷For example in Ref. [78], the transformation $\check{L} \bar{\sigma}_3(\cdot) \check{L}$ on the Green's function is performed. Here the matrix $\bar{\sigma}_3$ has been included in the definition of \check{G}_{ur} .

Green's function. When calculating observables, a specific representation for \check{G} is chosen.

Below, the derivation of the equation of motion for the quasiclassical Green's function, the Usadel equation, is summarized in Keldysh formalism. The starting point is the Dyson equation for \check{G} , which is called the Gor'kov equation [4, 80]

$$\int d1' (\check{G}_0^{-1} - \check{\Delta} - \check{\Sigma})(1, 1')\check{G}(1', 2) = \delta(1 - 2)\hat{\tau}_0 \otimes \bar{\sigma}_0. \quad (3.6)$$

In this formula, the operator $\check{G}_0^{-1}(1, 2) = \delta(1 - 2)\hat{\tau}_0 \otimes \bar{\sigma}_0 \left(i\hat{\tau}_3 \frac{\partial}{\partial t_1} + \frac{\nabla_1^2}{2m} - e\phi(1) + \mu \right)$ describes the scattering-free propagation of the electrons while $\hat{\tau}_3$ is the third Pauli matrix. The external potential ϕ is assumed to vary only on the length scales much larger than the Fermi wavelength, and the chemical potential is denoted by μ . The self-energy $\check{\Sigma}$ describes the scattering which is here assumed to be elastic. The pair-potential matrix related to superconductivity is of the form

$$\check{\Delta}(1, 2) = \delta(1 - 2) \begin{pmatrix} 0 & \Delta(1) \\ \Delta^*(1) & 0 \end{pmatrix} \otimes \sigma_0. \quad (3.7)$$

The Green's function $\check{G}(1, 2)$ oscillates rapidly as a function of the relative coordinate $\Delta\mathbf{r} = \mathbf{r}_2 - \mathbf{r}_1$, and its Wigner transformation $\check{G}(\mathbf{p}, \mathbf{r}; t, t')$, which is a function of the center of mass momentum and position, \mathbf{p} and \mathbf{r} , is strongly peaked at \mathbf{p} near the Fermi surface. If the interference effects second order in ε/E_F are ignored the information contained in these oscillations may be neglected. Hence it is natural to eliminate the dependence on the magnitude of the momentum and integrate the Green's function over $\xi_p \equiv p^2/2m - \mu$. This yields the quasiclassical Green's function [72, 78, 79, 81–83]

$$\tilde{g}(\mathbf{r}, \mathbf{v}_F; \varepsilon) = \frac{i}{\pi} \int d\xi_p \check{G}(\xi_p, \mathbf{v}_F, \mathbf{r}; \varepsilon). \quad (3.8)$$

Here a stationary case has been assumed and the Fourier transformation from $t_2 - t_1$ to energy ε has been performed but the quasiclassical approximation does not involve the temporal coordinates. With momenta far from the Fermi surface, $\check{G}(\xi_p, \mathbf{v}_F, \mathbf{r}; \varepsilon)$ is dominated by terms $\sim 1/\xi_p$. They contribute, e.g., to the electron density, but are not altered when the system is driven out of equilibrium. These terms are irrelevant

for the transport characteristics and the integration f performed along a specific contour [78, 82, 84] neglects them.

For conventional superconductors the dimensionless parameter Δ/E_F is of the order of 10^{-3} . Hence the superconducting coherence length ξ_S is much larger than λ_F , and at sufficiently low temperatures and voltages the dispersion relation around the Fermi energy for the quasiparticles is linear. Under these conditions the Eilenberger equation [84]

$$\mathbf{v}_F \cdot \nabla \tilde{g}(\mathbf{r}, \mathbf{v}_F; \varepsilon) = [-i\varepsilon\check{\tau}_3 + i\check{\sigma}(\mathbf{r}, \mathbf{v}_F; \varepsilon), \tilde{g}(\mathbf{r}, \mathbf{v}_F; \varepsilon)] \quad (3.9)$$

follows from the Gor'kov equation (3.6). Here $\check{\tau}_3$ is the matrix $\check{\tau}_3 = \hat{\tau}_3 \otimes \bar{\sigma}_0$. For later convenience, a new kind of self-energy term $\check{\sigma}(\mathbf{r}, \mathbf{v}_F; \varepsilon) = \check{\Delta} - i\langle \tilde{g} \rangle_{\mathbf{p}_F} / 2\tau_{\text{el}}$ has been introduced. Here the last term follows from the Born approximation. In the dirty limit, i.e., when $\check{\sigma}$ is dominated by strong elastic scattering with $1/\tau_{\text{el}} \gg E_T, \Delta, eV, T$, the Green's function \tilde{g} is nearly isotropic. It may be expanded in spherical harmonics $\tilde{g} = \check{g} + \mathbf{v}_F \cdot \check{\mathbf{g}}_p$ such that \check{g} and $\check{\mathbf{g}}_p$ denote the s -wave and p -wave components. The self-energy is then $\check{\sigma}(\mathbf{r}; \varepsilon) = \check{\Delta}(\mathbf{r}) - i\check{g}(\mathbf{r})/2\tau_{\text{el}}$. Furthermore, \check{g} , and thus also \check{g} , obeys the normalization condition $\check{g}^2 = \check{g}^2 = \hat{\tau}_0 \otimes \bar{\sigma}_0$ reflecting the conservation of probability. Multiplying the Eilenberger equation (3.9) by \mathbf{v}_F and taking the angular average over its direction gives $\check{\mathbf{g}}_p = \tau_{\text{el}}\check{g}\nabla\check{g}$. Substituting this into Eq. (3.9) and taking the angular average yields the Usadel equation

$$-\frac{D}{\sigma}\nabla \cdot \check{j}(x) \equiv D\nabla \cdot (\check{g}(\mathbf{r}, \varepsilon)\nabla\check{g}(\mathbf{r}, \varepsilon)) = [-i\varepsilon\check{\tau}_3 + \check{\Delta}(\mathbf{r}), \check{g}(\mathbf{r}, \varepsilon)]. \quad (3.10)$$

Here the matrix current density $\check{j}(\mathbf{r}) \equiv -\sigma\check{g}(\mathbf{r})\nabla\check{g}(\mathbf{r})$ has been introduced. The diffusion coefficient $D = v_F^2\tau_{\text{el}}/3$ has been assumed to be constant in space, $\sigma = 2e^2N_0D$ is the normal-state Drude conductivity and N_0 is the normal-state density of states. In a quasi-one-dimensional diffusive wire with length L and cross section A the matrix current equals $\check{J}(x) \equiv A\check{j}(x) = -LG_D\check{g}(x)\partial_x\check{g}(x)$. Here $G_D = \sigma A/L$ is the normal-state conductance of the wire and x the spatial coordinate along the wire.

The Usadel equation (3.10) is based on the assumption that \check{g} varies smoothly on the length scale of l_{el} . At the boundaries where \check{g} changes rapidly, e.g., at the

interface with a tunnel barrier created by an oxide layer, or at the interface of two different metals, the behavior of \check{g} may be treated with the help of the boundary conditions. The Nazarov boundary conditions [85] yield the matrix current through the interface from the left-hand side (with the Green's function \check{g}_L) to the right-hand side (with the Green's function \check{g}_R)

$$\check{J}_{L \rightarrow R} = -\frac{e^2}{\pi} \sum_n \frac{2T_n[\check{g}_L, \check{g}_R]}{4 + T_n[\{\check{g}_L, \check{g}_R\} - 2]}. \quad (3.11)$$

Here $\{T_n\}$ are the eigenvalues of the transmission matrix (cf. Subs. 4.1) through the interface. The derivation of Eq. (3.11) employs the normalization of \check{g} but does not assume any specific matrix structure. When the contact resistance $1/G_B$ through the interface is much smaller than the resistance $1/G_D$ of the wire the boundary conditions may be deduced from the continuity of \check{g} .

With the Keldysh rotation, \check{g} is cast to a triangular form in Keldysh space. Equation (3.5) is also valid with the substitutions $\check{G}(1, 1') \rightarrow \check{g}(\mathbf{r}_1)$, $\hat{G}^R(1, 1') \rightarrow \hat{R}(\mathbf{r}_1)$, etc. The retarded part \hat{R} may be represented by two complex parameters, θ and ϕ , characterizing the magnitude and phase of the electron-hole correlations [72]

$$\hat{R} = \cosh(\theta)\hat{\tau}_3 + \sinh(\theta)(\cos(\phi)i\hat{\tau}_2 + \sin(\phi)i\hat{\tau}_1). \quad (3.12)$$

By their definition, the retarded and advanced Green's functions are related by the retarded-advanced symmetry $\hat{A} = -\hat{\tau}_3\hat{R}^\dagger\hat{\tau}_3$. The distributions of the electrons and holes are contained in \hat{K} and can be treated by dividing the functions into even and odd components with respect to Fermi surface, f_T and f_L

$$\hat{K} = \hat{R}\hat{h} - \hat{h}\hat{A}, \quad \hat{h} = f_L + f_T\hat{\tau}_3. \quad (3.13)$$

The even part $f_T = 1 - f(eV - \varepsilon) - f(eV + \varepsilon)$ describes the imbalance between the hole $[1 - f(eV - \varepsilon)]$ and electron $[f(eV + \varepsilon)]$ distributions. The odd part $f_L = f(eV - \varepsilon) - f(eV + \varepsilon)$ characterizes the occupation of the electron-hole-pair states. With this parametrization, at equilibrium with temperature T and potential V , the definition of \check{g} yields in a normal bulk metal

$$\check{g}_N = \begin{pmatrix} \hat{\tau}_3 & 2\hat{h}_N\hat{\tau}_3 \\ \hat{0} & -\hat{\tau}_3 \end{pmatrix}, \quad \hat{h}_N = \begin{pmatrix} 1 - 2f_{N0}(\varepsilon + eV) & 0 \\ 0 & 2f_{N0}(-\varepsilon + eV) - 1 \end{pmatrix}, \quad (3.14)$$

with $f_{N0}(\varepsilon + eV) = 1/\{1 + \exp[(\varepsilon + eV)/T]\}$ the usual Fermi distribution function. This implies $f_{T(L)} = \{\tanh[(\varepsilon + eV)/2T] \pm \tanh[(\varepsilon - eV)/2T]\}/2$ in equilibrium. At a superconducting terminal one has

$$\check{g}_S = \frac{|\varepsilon|}{\sqrt{\varepsilon^2 - |\Delta|^2}} \begin{pmatrix} \hat{R}_S & (1 - \text{sgn}(|\Delta| - |\varepsilon|))\hat{R}_S f_L \\ \hat{0} & \text{sgn}(|\Delta| - |\varepsilon|)\hat{R}_S \end{pmatrix}, \quad \hat{R}_S = \hat{\tau}_3 + |\Delta|e^{i\hat{\tau}_3\phi}i\hat{\tau}_2/\varepsilon. \quad (3.15)$$

At the NS interface with $G_B \gg G_N$, the distribution of particle-like excitations equals that of holes and one has $f_T = 0$. Moreover, the Nazarov boundary conditions imply $\partial_x f_L(x) = 0$ across the NS interface, which reflects the fact that the thermal current into a bulk superconductor vanishes [cf. Eqs. (3.17) and (3.21)].

The retarded and advanced parts of the Usadel matrix equation (3.10) for \check{g} are equivalent to two coupled complex differential equations for θ and ϕ , which in a normal metal read

$$\begin{aligned} D\nabla^2\theta &= -2i\varepsilon \sinh\theta + \frac{D}{2}(\nabla\phi)^2 \sinh(2\theta), \\ \nabla \cdot \mathbf{j}_E &= 0, \quad \mathbf{j}_E = -\sinh^2\theta \nabla\phi. \end{aligned} \quad (3.16)$$

The electrons and holes have slightly different energies around the Fermi surface and their dephasing is described by the first equation. The second equation is the conservation law for a spectral supercurrent \mathbf{j}_E . The kinetic variables $f_{T,L}$ obey two coupled real linear equations

$$\nabla \cdot \mathbf{j}_L = 0, \quad \mathbf{j}_L = \mathcal{D}_L \nabla f_L - \mathcal{T} \nabla f_T + j_S f_T, \quad (3.17)$$

$$\nabla \cdot \mathbf{j}_T = 0, \quad \mathbf{j}_T = \mathcal{D}_T \nabla f_T + \mathcal{T} \nabla f_L + j_S f_L, \quad (3.18)$$

where j_S is given by $j_S = \text{Im}(\mathbf{j}_E)$ and also the coefficients $\mathcal{D}_{L,T}, \mathcal{T}$ are functions of the spectral variables (see Ref. [86]). The conserved quantities $\mathbf{j}_{T,L}$ may be interpreted as spectral charge and energy current densities.

Starting from the definitions, the time-independent charge current density for spin-degenerate electrons in a diffusive wire with length L and cross section A may

be calculated as follows

$$\begin{aligned}
\mathbf{j}_c &= \frac{i\hbar e}{2m}(\nabla_1 - \nabla_2)\text{Tr}\langle\hat{\tau}_3\hat{\Psi}^\dagger(\mathbf{r}_2, t) \otimes \hat{\Psi}(\mathbf{r}_1, t)\rangle|_{\mathbf{r}_1=\mathbf{r}_2} = \frac{e\hbar}{4m}\nabla_{\Delta\mathbf{r}}\text{Tr}[\check{\tau}_K\check{G}(\Delta\mathbf{r}, \mathbf{r}, \Delta t)]|_{\Delta\mathbf{r}=0, \Delta t=0+} \\
&= -\frac{eN_0}{2}\int d\xi_p \int \frac{d\Omega_p}{4\pi} \int \frac{d\varepsilon}{2\pi} \mathbf{v}\text{Tr} [i\check{\tau}_K\check{G}(\xi_p, \mathbf{v}, \mathbf{r}, \varepsilon)] \\
&= -\frac{eN_0}{4}\int d\varepsilon \int \frac{d\Omega_p}{4\pi} \mathbf{v}_F\text{Tr}[\check{\tau}_K\check{g}(\mathbf{r}, \mathbf{v}_F, \varepsilon)] = \frac{G_D L}{8eA} \int d\varepsilon \text{Tr}[\check{\tau}_K\check{g}(\mathbf{r}, \varepsilon)\nabla\check{g}(\mathbf{r}, \varepsilon)]
\end{aligned} \tag{3.19}$$

In the first equality, the factor 2 has been inserted for spin degeneracy. The factor 1/2 arises once from the symmetrization with respect to spatial coordinates and once more because the field operators take into account both the particle and hole contributions [cf. Eq. (3.2)]. In the last expression on the first line, $\check{\tau}_K$ depends on the representation of \check{G} . In order to make connection with the Keldysh structure, the equality $i\langle\hat{\Psi}^\dagger(2) \otimes \hat{\Psi}(1)\rangle = [\hat{K} + (\hat{R} - \hat{A})](2, 1)/2$ is used. The term $\hat{R} - \hat{A}$ does not contribute to the nonequilibrium current since it only depends on the equilibrium properties of the system. Thus with \check{G} equal to \check{G}_{rot} [cf. Eq. (3.5)] the physical current is obtained by picking the Keldysh component and taking the trace $\text{Tr}[\check{\tau}_K(\cdot)]$ with $\check{\tau}_K = \hat{\tau}_3 \otimes \bar{\sigma}_1$. With $\check{G} = \check{G}_{\text{ur}}$ [cf. Eq. (3.4)], on the other hand, $\check{\tau}_K = \hat{\tau}_3 \otimes \bar{\sigma}_3$ may be used due to the identity $\hat{K}(1, 2) \equiv -i\langle[\hat{\Psi}(1) \otimes \hat{\Psi}^\dagger(2)]\rangle = -i(\langle\vec{T}\hat{\Psi}(1) \otimes \hat{\Psi}^\dagger(2)\rangle + \langle\overleftarrow{T}\hat{\Psi}(1) \otimes \hat{\Psi}^\dagger(2)\rangle)$. On the second line the gradient with respect to the relative coordinate has been expressed in terms of the center-of-mass velocity, \mathbf{v} . On the third line, the quasiclassical approximation has been adopted and the contribution of the momenta far from the Fermi surface, which do not contribute to the current, has been neglected. In the last equality, the diffusive approximation in a diffusive wire has been employed, and the matrix current density $\check{j} = -\sigma_N\check{g}(\mathbf{r}, \varepsilon)\nabla\check{g}(\mathbf{r}, \varepsilon)$ may be identified in the final form. For the energy current \mathbf{j}_Q an analogous expression may be derived.

Putting all together, in the parametrization chosen in Eqs. (3.16)–(3.18) the observable charge and energy currents are given by

$$\mathbf{j}_c = -\frac{1}{8e} \int d\varepsilon \text{Tr}[\check{\tau}_K\check{j}] = \frac{\sigma_N}{2e} \int_{-\infty}^{\infty} d\varepsilon \mathbf{j}_T, \tag{3.20}$$

$$\mathbf{j}_Q = -\frac{1}{8e^2} \int d\varepsilon \varepsilon \text{Tr}[\check{\tau}_K\check{j}] = \frac{\sigma_N}{2e^2} \int_{-\infty}^{\infty} d\varepsilon \varepsilon \mathbf{j}_L. \tag{3.21}$$

Thus the conserved quantities \mathbf{j}_T and \mathbf{j}_L in Eqs. (3.17) and (3.18) are the spectral charge and energy current densities. Their first two terms constitute the dissipative part and the last ones are the supercurrent parts. The local chemical potential $\mu(x)$ may be defined through the condition that \mathbf{j}_c through the probe connected to the terminal with the chemical potential μ , and at a position x to a mesoscopic wire, vanishes with $\mu(x) = \mu$. In a normal-metal terminal, the equilibrium form of f_T [cf. Eq. (3.14)] yields $\int_{-\infty}^{\infty} d\varepsilon f_T = 2\mu$. Since in the absence of superconductivity \mathcal{T} and j_S vanish, Eqs. (3.18) and (3.20) imply $\mu(x) = \int_0^{\infty} d\varepsilon f_T(x)$ in a wire. In an analogous way it may be shown that the deviation of f_L from its equilibrium value is related to the local effective temperature [87].

3.2.1 Full counting statistics

Consider the electrons transmitted through mesoscopic conductors and being measured in terminals $\{T_j\}$. The numbers $\mathbf{N} \equiv (\dots, N_j, \dots)$ of particles transferred in unit time t_0 vary due to the quantum nature of the transport process and may be assigned a probability $P_{t_0}(\mathbf{N})$. The full counting statistics [88–91] has recently become the method of choice to study the current distribution in mesoscopic conductors. The current distribution $P_{t_0}(\mathbf{N})$ is conveniently discussed through its Fourier transform and the cumulant generating function $\tilde{S}(\boldsymbol{\chi})$

$$\exp(-\tilde{S}(\boldsymbol{\chi})) \equiv \sum_{\mathbf{N}} P_{t_0}(\mathbf{N}) \exp(i\mathbf{N} \cdot \boldsymbol{\chi}) = \langle \overrightarrow{T} e^{(-i/2e) \int_0^{t_0} dt \boldsymbol{\chi} \cdot \hat{\mathbf{I}}(t)} \overleftarrow{T} e^{(-i/2e) \int_0^{t_0} dt \boldsymbol{\chi} \cdot \hat{\mathbf{I}}(t)} \rangle. \quad (3.22)$$

Here $\boldsymbol{\chi} \equiv (\dots, \chi_j, \dots)^T$ is called the counting field, the component χ_j is associated with the number of particles measured in terminal T_j , and $\hat{\mathbf{I}} = (\dots, \hat{I}_j, \dots)^T$ contains the current operators for the currents flowing into the terminals. The time-ordering and anti-timeordering operators are denoted by \overrightarrow{T} and \overleftarrow{T} , respectively. The n th current cumulant measured in terminal T_j is obtained from

$$C_{n,j} = - \left. \frac{\partial^n \tilde{S}(\boldsymbol{\chi})}{\partial (i\chi_j)^n} \right|_{\boldsymbol{\chi}=0}. \quad (3.23)$$

The first and second cumulants are directly related to average current and shot noise, respectively, while the higher cumulants measure the deviation of $P_{t_0}(N)$

from the Gaussian form, cf. Subs. 2.7. The cumulant generating function $\tilde{S}(\boldsymbol{\chi})$ may be expressed through a generalized Green's function $\check{g}(\mathbf{r}, \boldsymbol{\chi})$. This Green's function still satisfies the Usadel equation (3.10) in diffusive wires and the Nazarov boundary conditions (3.11) at interfaces but its values in terminals are different from $\check{g}(\mathbf{r})$.

By the definition (3.22), the CGF measured in a certain terminal may be accessed by the Green's function $\check{G}(1, 1'; \boldsymbol{\chi})$ satisfying the following equation of motion [88, 90, 92]

$$\left[i \frac{\partial}{\partial t_1} - \check{H}(1) + \frac{\chi_j}{2e} \check{\tau}_K (\nabla F_j(\mathbf{r}_1)) \cdot \lim_{\mathbf{r}_1 \rightarrow \mathbf{r}'_1} \frac{e}{2m} (\nabla_{\mathbf{r}_1} - \nabla_{\mathbf{r}'_1}) \right] \check{G}(1, 1'; \boldsymbol{\chi}) = \delta(1 - 1') \quad (3.24)$$

The function $F_j(\mathbf{r}_1)$ has to be such that it changes smoothly from 1 to 0 across some surface B_j inside the terminal T_j (Fig. 3.2). Provided $F_j(\mathbf{x})$ changes from 1 to 0 on

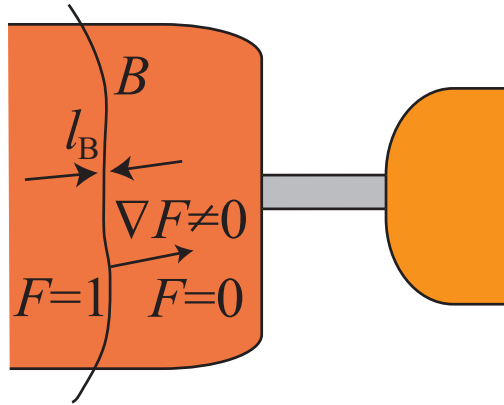


Figure 3.2: Charge counter measuring the current statistics in a terminal. The explicit dependence of the equations of motion from the component χ_j of the counting field (see text) may be eliminated by performing a counting rotation (3.25) on the Green's function in the terminal T_j . The value of function F changes from 1 to 0 across the boundary B on a length scale l_B .

the length scale l_B with $\lambda_F \ll l_B \ll l_{el}, \xi_S$, the quasiclassical equations of motion for the Green's function $\check{g}(\mathbf{r}, \varepsilon, \boldsymbol{\chi})$ may be employed so that it satisfies near B_j the Eilenberger equation Eq. (3.9) with the self-energy $\check{\sigma} = -\chi_j \nabla(F_j(\mathbf{x})) \cdot \mathbf{v}_F \check{\tau}_K / 2$. Since $F_j(\mathbf{x})$ vanishes inside the wires, the Eilenberger equation may be solved by

performing a gauge transformation [90]

$$\tilde{g}(\mathbf{r}, \mathbf{v}_F, \varepsilon, \boldsymbol{\chi}) = e^{-i\chi_j F_j(\mathbf{r})\tilde{\tau}_K/2} \tilde{g}(\mathbf{r}, \mathbf{v}_F, \varepsilon, \boldsymbol{\chi} = 0) e^{i\chi_j F_j(\mathbf{r})\tilde{\tau}_K/2} \quad (3.25)$$

on the Green's function in each terminal T_j . In the diffusive approximation $\check{g}(\mathbf{r}, \varepsilon, \boldsymbol{\chi})$ thus satisfies the Usadel equation (3.10) in the wires. At the interfaces the Nazarov boundary conditions (3.11) for $\check{g}(\mathbf{r}, \varepsilon, \boldsymbol{\chi})$ hold, since their derivation, originally carried out for $\check{g}(\mathbf{r}, \varepsilon, \boldsymbol{\chi} = 0)$, does not assume any specific matrix structure for the quasiclassical Green's functions but only makes use of their normalization. Deep in the terminal T_j the value of $\check{g}(\mathbf{r}, \varepsilon, \boldsymbol{\chi})$ is obtained from Eq. (3.25) with the substitutions $\tilde{g}(\mathbf{r}, \mathbf{v}_F, \varepsilon, \boldsymbol{\chi}_j) \rightarrow \check{g}(\mathbf{r}, \varepsilon, \boldsymbol{\chi}_j)$, $F_j(\mathbf{r}) \rightarrow 1$.

The cumulant generating function $\tilde{S}(\boldsymbol{\chi})$ in the terminals and the Green's function $\check{g}(\mathbf{r}, \boldsymbol{\chi})$ in a wire connected to the terminal T_j are related by [90]

$$-\frac{\partial \tilde{S}(\boldsymbol{\chi})}{\partial (i\chi_j)} = \frac{t_0}{e} \frac{1}{8e} \int d\varepsilon \text{Tr}[\tilde{\tau}_K \check{J}_j(\boldsymbol{\chi})], \quad \check{J}_j(\boldsymbol{\chi}) \equiv -LG_D \check{g}(\mathbf{r}, \boldsymbol{\chi}) \nabla \check{g}(\mathbf{r}, \boldsymbol{\chi}). \quad (3.26)$$

This is obtained by considering the diagrammatic expansions of both sides of the equality [90] and making use of the linked cluster theorem [4]. The conserved quantity $J_j(\boldsymbol{\chi}) \equiv -\int d\varepsilon \text{Tr}[\tilde{\tau}_K \check{J}_j(\boldsymbol{\chi})]/8e$, which formally resembles electric current, is called the counting current and is in this equation to be evaluated in the wire connected to T_j .

3.2.2 Noise correlations

In metallic conductors, the corrections induced by quantum coherence are rather small, but in a metal in contact to a superconductor more pronounced effects may be observed, e.g., in the out-of-equilibrium noise experiments [93–96]. The voltage dependence of the shot noise in a two-terminal setup has been theoretically studied in Paper III and in Ref. [97]. Current fluctuations in multiterminal structures have been previously theoretically studied in the incoherent regime [92, 98–100], and in the presence of a supercurrent, in a short junction [101], and for specific values of a phase difference in a three-terminal setup. The latter was described by a method based on a direct discretization of the Usadel equation (3.10) [96]. In the following

we present a parametrization of the Usadel equation to calculate noise correlations in the presence of supercurrent.

Noise correlations are obtained from counting current through

$$S_{ij} \equiv \int_{-\infty}^{\infty} dt \langle \{\delta I_i(t), \delta I_j(0)\} \rangle = -2ie \frac{\partial J_i(\boldsymbol{\chi})}{\partial \chi_j} \Big|_{\boldsymbol{\chi}=0}. \quad (3.27)$$

Here $\delta I_i = I_i - \bar{I}_i$ is the deviation of the current from its quantum mechanical expectation value. The matrix current in the first order in χ_j

$$\check{J}^{(1,j)}(x) \equiv -2i \partial_{\chi_j} \check{J}(x) \Big|_{\boldsymbol{\chi}=0} = -LG_D(\check{g}_0 \partial_x \check{g}_{1,j} + \check{g}_{1,j} \partial_x \check{g}_0) \quad (3.28)$$

is defined so that the Usadel equation in the first order in χ_j is identical to Eq. (3.10) with the substitution $\check{g} \rightarrow \check{g}_{1,j}, \check{j} \rightarrow \check{j}^{(1,j)} = \check{J}^{(1,j)}/A$. Here the notation $\check{g}_0 \equiv \check{g}(\chi = 0)$, $\check{g}_{1,j} \equiv 2i \partial_{\chi_j} \check{g}(\chi) \Big|_{\boldsymbol{\chi}=0}$ has been introduced. With $i \neq j$ the Nazarov boundary conditions for $\check{J}^{(1,j)}$ through the interface to the terminal with the Green's function \check{g}_T are given by [73]⁸

$$\begin{aligned} \check{J}^{(1,j)} &= -2G_B \frac{\sum_n T_n \check{A} \check{B} \check{A}}{\sum_n T_n}, \quad \check{A} = [4 + T_n(\{\check{g}_0, \check{g}_T\} - 2)]^{-1}, \\ \check{B} &= 4[\check{g}_{1,j}, \check{g}_T] + 2T_n(\check{g}_T \check{g}_0 \check{g}_{1,j} \check{g}_T - \check{g}_0 \check{g}_{1,j} - [\check{g}_{1,j}, \check{g}_T]). \end{aligned} \quad (3.29)$$

Here $\{T_n\}$ are the eigenvalues of the transmission matrix through the interface, with conductance $G_B = e^2 \sum_n T_n / \pi$. The normalization of $\check{g}(\chi)$ implies $\{\check{g}_0(x), \check{g}_1(x)\} = 0$. This is readily satisfied by introducing the change of the variables $\check{g}_1(x) = \{\check{g}_0(x), \check{\phi}(x)\}$ ⁹.

We find a parametrization for $\check{\phi}(x)$ valid also in the presence of a supercurrent (see Paper II)

$$\check{\phi} = \begin{pmatrix} \hat{r} & \hat{k} \\ \hat{l} & \hat{a} \end{pmatrix} = \begin{pmatrix} r_1 \hat{\tau}_1 + r_3 \hat{\tau}_3 & k_0 \hat{\tau}_0 + k_3 \hat{\tau}_3 \\ f_L \hat{\tau}_0 - f_T \hat{\tau}_3 & r_1^* \hat{\tau}_1 - r_3^* \hat{\tau}_3 \end{pmatrix}, \quad (3.30)$$

with $r_1 = r_{11} + r_{12}i$, $r_3 = r_{31} + r_{32}i$, and $r_{11}, r_{12}, r_{31}, r_{32}, k_0, k_3 \in \Re$. With this parametrization, χ has to be generated in the normal terminal and an arbitrary number of superconducting terminals be at zero potential. With $i \neq j$ the boundary conditions for the parameters are obtained from Eq. (3.29), and for $i = j$, in a good

⁸There is a misprint in Eq. (3.29) in Ref. [73].

⁹For clarity the subindex j is dropped here.

contact, from $\check{g}_{1,j} = [\check{\tau}_K, \check{g}_{N,0}]$ with $\check{\tau}_K = \hat{\tau}_3 \otimes \bar{\sigma}_1$. On the other hand, for example, in a case of several normal terminals, the boundary conditions would imply a vanishing $\check{g}_{1,j}$ at a good contact between a wire and a normal terminal other than the one generating χ_j , which would not be compatible with the parametrization (3.30).

Not all the coefficients in the retarded part of the Usadel equation are independent but the equations take the form

$$\begin{aligned}
& \mathcal{R}_{11}^{(2)} r''_{11} + \mathcal{R}_{11}^{(1)} r'_{11} + \mathcal{R}_{11}^{(0)} r_{11} + \mathcal{R}_{12}^{(2)} r''_{12} + \mathcal{R}_{12}^{(1)} r'_{12} + \mathcal{R}_{12}^{(0)} r_{12} + \mathcal{R}_{31}^{(2)} r''_{31} + \mathcal{R}_{31}^{(1)} r'_{31} \\
& \qquad \qquad \qquad + \mathcal{R}_{32}^{(2)} r''_{32} + \mathcal{R}_{32}^{(1)} r'_{32} = \mathcal{C}_1, \\
& -\mathcal{R}_{21}^{(2)} r''_{11} - \mathcal{R}_{12}^{(1)} r'_{11} - \mathcal{R}_{11}^{(0)} r_{11} + \mathcal{R}_{11}^{(2)} r''_{12} + \mathcal{R}_{11}^{(1)} r'_{12} + \mathcal{R}_{11}^{(0)} r_{12} - \mathcal{R}_{32}^{(2)} r''_{31} - \mathcal{R}_{32}^{(1)} r'_{31} \\
& \qquad \qquad \qquad + \mathcal{R}_{31}^{(2)} r''_{32} + \mathcal{R}_{31}^{(1)} r'_{32} = \mathcal{C}_2, \\
& \mathcal{R}_{31}^{(2)} r''_{11} + \mathcal{P}_{11}^{(1)} r'_{11} + \mathcal{P}_{11}^{(0)} r_{11} + \mathcal{R}_{32}^{(2)} r''_{12} + \mathcal{P}_{12}^{(1)} r'_{12} + \mathcal{P}_{12}^{(0)} r_{12} + \mathcal{P}_{31}^{(2)} r''_{31} + \mathcal{P}_{31}^{(1)} r'_{31} \\
& \qquad \qquad \qquad + \mathcal{P}_{32}^{(2)} r''_{32} + \mathcal{P}_{32}^{(1)} r'_{32} = \mathcal{C}_3, \\
& -\mathcal{R}_{32}^{(2)} r''_{11} - \mathcal{P}_{12}^{(1)} r'_{11} - \mathcal{P}_{12}^{(0)} r_{11} + \mathcal{R}_{31}^{(2)} r''_{12} + \mathcal{P}_{11}^{(1)} r'_{12} + \mathcal{P}_{11}^{(0)} r_{12} - \mathcal{P}_{32}^{(2)} r''_{31} - \mathcal{P}_{32}^{(1)} r'_{31} \\
& \qquad \qquad \qquad + \mathcal{P}_{31}^{(2)} r''_{32} + \mathcal{P}_{31}^{(1)} r'_{32} = \mathcal{C}_4.
\end{aligned} \tag{3.31}$$

Here $\mathcal{R}_{ij}^{(k)}$, $\mathcal{P}_{ij}^{(k)}$, $\mathcal{C}_i \in \mathfrak{R}$ depend on $\theta, \phi, f_{L,T}$ and their derivatives and are obtained by direct calculation from the Usadel equation. These expressions are, however, too long to write here. The Keldysh part obeys two coupled differential equations

$$\begin{aligned}
& \mathcal{K}_0^{(2)} k''_0 + \mathcal{K}_0^{(1)} k'_0 + \mathcal{K}_3^{(2)} k''_3 + \mathcal{K}_3^{(1)} k'_3 = \mathcal{S}_1, \\
& -\mathcal{K}_0^{(2)} k''_0 + \mathcal{Q}_0^{(1)} k'_0 + \mathcal{Q}_3^{(2)} k''_3 + \mathcal{Q}_3^{(1)} k'_3 = \mathcal{S}_2.
\end{aligned} \tag{3.32}$$

Here $\mathcal{K}_{0,3}^{(1,2)}$, $\mathcal{Q}_{0,3}^{(1,2)}$, $\mathcal{S}_{1,2} \in \mathfrak{R}$ depend on $\theta, \phi, f_{L,T}, r_{1,3}$ and their derivatives and are also obtained from the Usadel equation.

Putting all together, the spectral equations for θ, ϕ and the kinetic equations for f_L, f_T are first solved, then Eq. (3.31) for r_1, r_3 , and thereafter Eq. (3.32) for k_0, k_3 . Equations (3.27) and (3.28) yield an expression for noise correlations into which the values of these parameters are finally substituted. Such calculations were carried out in Paper II.

4 Random matrix theory

Compared to the Nambu-Keldysh method of Sec. 3, the methods based on the random matrix theory and the Dorokhov-Mello-Pereyra-Kumar (DMPK) equation (introduced in Subs. 4.2) have an advantage of being applicable to the localization behavior (both weak and strong) of electronic states and the fluctuations of conductance around the mean. Random matrix theory can also be used, e.g., to derive the distribution of transmission eigenvalues T_n appearing in the Nazarov boundary conditions (3.11). Below in Subs. 4.1 we introduce the general scattering matrix theory that is the basis for the random matrix theory, the DMPK equation, and the numerical scattering approach of Sec. 5. The DMPK equation for the standard and the so-called BdG symmetry classes is the starting point for the calculations in Paper I.

4.1 Scattering theory

The Landauer-Büttiker formalism [11] describes a scattering area connected to quasiparticle reservoirs by ideal crystalline leads (see Fig. 4.1). The incoming and

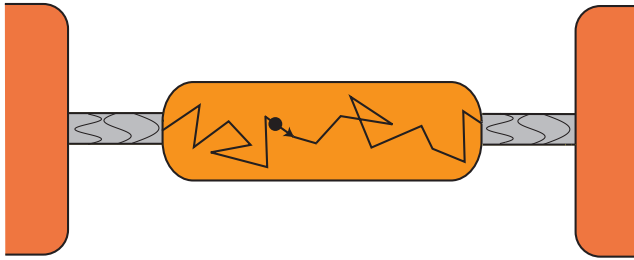


Figure 4.1: Scattering area coupled to two terminals through crystalline leads.

outgoing quasiparticle fluxes are characterized by the vectors \mathbf{a}^{in} and \mathbf{a}^{out} of complex amplitudes such that the total flux is normalized to unity. For example $\mathbf{a}^{\text{in}} \equiv (\mathbf{a}^{\text{in,L}}, \mathbf{a}^{\text{in,R}})$, contains the incoming amplitudes on the left and right hand side, e.g., $\mathbf{a}^{\text{in,L}} = (a_1^{\text{in,L}}, \dots, a_{N_c}^{\text{in,L}})$. Here the subindices refer to the N_c transmission channels.

The scattering matrix S describes the transmissions and reflections between the quasiparticle states in the two leads through

$$\mathbf{a}^{\text{out}} = S\mathbf{a}^{\text{in}}, \quad S = \begin{pmatrix} r & t' \\ t & r' \end{pmatrix}. \quad (4.1)$$

For example, in a normal metal, the differential conductance and shot noise may be expressed through [15, 102]

$$G = \frac{dI}{dV} = \frac{2e^2}{h} \sum_{\alpha} T_{\alpha}, \quad \frac{dS}{dV} = \frac{4e^2}{h} \sum_{\alpha} T_{\alpha}(1 - T_{\alpha}). \quad (4.2)$$

Here the probabilities T_{α} are the eigenvalues of the matrix tt^{\dagger} .

An equivalent approach is to consider the transfer matrix M which relates $\mathbf{a}^{\text{L}} = (a_1^{\text{in,L}}, \dots, a_{N_c}^{\text{in,L}}, a_1^{\text{out,L}}, \dots, a_{N_c}^{\text{out,L}})$ and \mathbf{a}^{R} through $\mathbf{a}^{\text{R}} = M\mathbf{a}^{\text{L}}$. The transfer matrices have the advantage of obeying a simple composition rule. When two scattering areas with transfer matrices M_1 and M_2 are combined, the resulting transfer matrix equals M_1M_2 .

A given transfer matrix M may be parametrized through the polar decomposition¹⁰ [63, 68, 103]

$$M = \begin{pmatrix} u^{(1)} & 0 \\ 0 & u^{(3)} \end{pmatrix} \begin{pmatrix} \sqrt{I + \Lambda} & \sqrt{\Lambda} \\ \sqrt{\Lambda} & \sqrt{I + \Lambda} \end{pmatrix} \begin{pmatrix} u^{(2)} & 0 \\ 0 & u^{(4)} \end{pmatrix} \equiv UGV. \quad (4.3)$$

Here $\Lambda \equiv \text{diag}(\lambda_1, \dots, \lambda_{N_c})$ with $\lambda_{\alpha} \equiv (1 - T_{\alpha})/T_{\alpha}$ describes the transmission eigenvalues while the remaining phase factors are contained in U and V . The physical symmetries of the system can be directly related to the symmetries of the submatrices $u^{(i)}$. For example time-reversal symmetry implies $u^{(3)} = u^{(1)*}$, $u^{(4)} = u^{(2)*}$.

4.2 Dorokhov-Mello-Pereyra-Kumar equation

Mesoscopic samples contain different kinds of nonidealities: impurity atoms, lattice dislocations, surface roughness etc. It is natural to examine the characteristics of an ensemble of conductors, and hence treat transfer and scattering matrices as random

¹⁰This is because current conservation implies "pseudo-unitarity" of M , i.e., $\Sigma_z M^{-1} \Sigma_z = M^{\dagger}$. Here Σ_z is a diagonal matrix with the elements $(\Sigma_z)_{nn} = 1$ for $1 \leq n \leq N_c$ and $(\Sigma_z)_{nn} = -1$ for $N_c + 1 \leq n \leq 2N_c$

Class	TR	SR	m_0	m_l	d
Standard	Yes	Yes	1	1	2
	No	Yes (No)	2	1	2(1)
	Yes	No	4	1	2
BdG	Yes	Yes	2	2	4
	No	Yes	4	3	4
	Yes	No	2	0	2
	No	No	1	0	1

Table 4.1: Classification of symmetry classes. The symmetry classes discussed in Paper I are classified according to the fundamental symmetries of the system (standard or BdG), and in terms of the presence or absence of time-reversal (TR) and spin-rotation (SR) symmetry. Parameters m_0 and m_l characterizing symmetries appear, for example, in the DMPK equation (4.8). The degeneracy d of the transmission eigenvalues stems from the spin degree of freedom for standard classes, and for the BdG classes from the particle type (electron or hole) and spin.

quantities obeying some general properties¹¹ [104, 106–109]. There exists altogether ten different symmetry classes [110] of which seven (see Table 4.1) are studied in Paper I. The standard classes refer to quantum transport in normal metals [104]. The BdG classes may be applied, e.g., for normal metals in contact to a superconductor [111, 112] or for the so-called ”disorder facilitated” heat transport in unconventional superconductors [113, 114].

The Dorokhov-Mello-Pereyra-Kumar (DMPK) equation [62, 103, 115] describes the evolution of the distribution function $w_L(\boldsymbol{\lambda})$ of the parameters $\boldsymbol{\lambda} = (\lambda_1, \dots, \lambda_{N_c})$, with increasing wire length L . The idea is that the transmission eigenvalues $\{T_i\}$ of a disordered wire undergo Brownian motion, i.e., ”walk” randomly, on the interval $[0, 1]$ as the length of the wire is altered. The main points of the derivation of the DMPK equation are sketched below.

¹¹Here the so-called local approach to random matrix theory is considered. The global approach [104] is not exact, and, even though originally believed so, is not equivalent to the local approach [105].

To begin with, distinct transfer matrices are supposed to be statistically independent

$$\tilde{p}_{L+\delta L}(M) = \int \tilde{p}_L(MM_{\delta L}^{-1})\tilde{p}_{\delta L}(M_{\delta L})d\tilde{\mu}(M_{\delta L}) \equiv \langle \tilde{p}_L(MM_{\delta L}^{-1}) \rangle_{\delta L}. \quad (4.4)$$

Here $\tilde{p}_L(M)$ is the probability density for the transfer matrices in a wire segment with length L . The measure $d\tilde{\mu}$

$$\begin{aligned} d\tilde{\mu}(M) &= \tilde{J}_{m_0}(\boldsymbol{\lambda}) \prod_a d\lambda_a \prod_i d\mu[u^{(i)}], \quad d\mu(u) = \prod_{a \leq b} \delta s_{ab} \prod_{c < d} \delta a_{cd}, \\ u^\dagger du &\equiv \delta a + i\delta s, \quad \tilde{J}_{m_0}(\boldsymbol{\lambda}) = \prod_{a < b} |\lambda_a - \lambda_b|^{m_0} \prod_c [\lambda_c(1 + \lambda_c)]^{(m_1-1)/2} \end{aligned} \quad (4.5)$$

is invariant under the multiplication of arbitrary transfer matrices M', M'' such that $d\tilde{\mu}(M) = d\tilde{\mu}(M'MM'')$. The first equality on the second line of Eq. (4.5) defines the matrices δs_{ab} and δa_{cd} (subindices refer to matrix elements, superscripts have been dropped for clarity). The probability density related to M may thus be obtained by considering the distribution of matrices Λ and the probability density $p_L(\Lambda)$. A small change in the length $\delta L \ll l_{\text{el}}$ of the wire may be expected to lead to a small change $\delta\lambda_a \ll 1$ in the parameters λ_a . So the changes $\delta\lambda_a$ may be calculated using perturbation theory. Expanding both sides of Eq. (4.4) yields

$$\begin{aligned} p_{L+\delta L}(\Lambda) &= p_L(\Lambda) + \frac{\partial p_L(\Lambda)}{\partial L} \delta L + \dots = \langle p_L(\Lambda + \delta\Lambda) \rangle_{\delta L} \\ &\approx p_L(\Lambda) + \sum_a \frac{\partial p_L(\Lambda)}{\partial \lambda_a} \underbrace{\langle \delta\lambda_a \rangle_{\delta L}}_{\sim \delta L} + \frac{1}{2} \sum_{ab} \frac{\partial^2 p_L(\Lambda)}{\partial \lambda_a \partial \lambda_b} \underbrace{\langle \delta\lambda_a \delta\lambda_b \rangle_{\delta L}}_{\sim \delta L + \mathcal{O}((\delta L)^2)}. \end{aligned} \quad (4.6)$$

Here the averages depend on the distributions of the matrices Λ and V of Eq. (4.3). The so-called "isotropy" assumption is used to decouple averages like $\langle u_{ca}^* u_{cb}^* u_{da} u_{db} \rangle \equiv \int (\dots) d\mu(u)$, from λ_i s.

For the distribution of matrices Λ , the starting point is the transmission eigenvalue distribution for a short wire segment with length $\delta L \ll l_{\text{el}}$. The average reflection probability is assumed to be linear in δL ¹². Moreover, the probability distribution of the transfer matrices for a short wire segment is assumed to maximize Shannon's information entropy [116]¹³. The distribution of matrices V can be

¹²The equality $\langle \text{Tr}(r^\dagger r) \rangle_{\delta L} = \langle \text{Tr}\Lambda \rangle_{\delta L} = N_c \delta L / l_{\text{el}}$, or equivalently, $\langle \text{Tr}(M^\dagger M) \rangle_{\delta L} = 2N_c(1 + \delta L / l_{\text{el}})$ is used.

¹³One has $\tilde{p}_{\delta L}(M) = \exp[-(N_c + 1)l_{\text{el}} \text{Tr}\Lambda / 2\delta L]$.

related to the physical symmetries of the system. For example, in a normal metal in the absence of the spin-orbit scattering, the matrices $u^{(i)}$ (cf. Eq. (4.3)) belong to the unitary group $\mathcal{U}(N)$ and for the averages of their products one has [117]

$$\begin{aligned} \langle u_{ab}u_{cd} \rangle &= \langle u_{ab}^*u_{cd}^* \rangle = 0, \quad \langle u_{ab}^*u_{cd} \rangle = \frac{1}{N_c}\delta_{ac}\delta_{bd}, \\ \langle u_{ca}^*u_{cb}^*u_{da}u_{db} \rangle &= \frac{(1+\delta_{ab})\delta_{cd}}{N_c(N_c+1)}, \quad \langle u_{ca}^*u_{ca}^*u_{db}u_{db} \rangle = \frac{2\delta_{ab}\delta_{cd}}{N_c(N_c+1)}. \end{aligned} \quad (4.7)$$

If the motion of the particles is ergodic, i.e., uniformly distributed over the phase space, these averages over the unitary group directly yield the correct expectation values in the corresponding ensemble. In quasi-one-dimension¹⁴, the motion of the particles is not uniformly distributed over the phase space but the ergodicity of the motion perpendicular to the wire length allows a random matrix theory to be applied. The last approximation (cf., marking \approx on the second line of Eq. 4.6) is to neglect in Eq. (4.6) the terms proportional to $\sum_{\alpha} \lambda_{\delta L, \alpha}^2$. These terms are small in a quasi-one-dimensional wire but not if the width of the wire is much larger than l_{el} [118]. Finally, one obtains a diffusion-like equation [62, 113, 114, 119]

$$\begin{aligned} \partial_s w_s(\boldsymbol{\lambda}) &= \frac{2N_c}{m_0 N_c + 1 + m_l - m_0} \sum_{i=1}^{N_c} \frac{\partial}{\partial \lambda_i} \left\{ [\lambda_i(1 + \lambda_i)]^{(m_l+1)/2} \right. \\ &\quad \left. \times J_{m_0}(\boldsymbol{\lambda}) \frac{\partial}{\partial \lambda_i} [\lambda_i(1 + \lambda_i)]^{(1-m_l)/2} \frac{w_s(\boldsymbol{\lambda})}{J_{m_0}(\boldsymbol{\lambda})} \right\}. \\ w_s(\boldsymbol{\lambda}) &= p_L(\Lambda) J_{m_0}(\boldsymbol{\lambda}), \quad J_{m_0}(\boldsymbol{\lambda}) = \prod_{a < b} |\lambda_a - \lambda_b|^{m_0}, \quad s \equiv L/N_c l. \end{aligned} \quad (4.8)$$

This is the Dorokhov-Mello-Pereyra-Kumar equation. In the DMPK equation, the number of transport channels N_c is a variable but one remarkable result obtained from the DMPK equation is also the one-parameter scaling equation for the transmission eigenvalue density for a large number of channels. As an example, the forms of the transmission eigenvalue distributions obtained from this equation in different regimes (ballistic, diffusive and localized) in normal-metal wire are illustrated in Fig. 4.2. These analytical solutions of the DMPK equation in the absence of weak (anti)localization in the large- N_c limit can be found in Refs. [68, 69] for the diffusive regime and in [120] for the ballistic and localized regimes.

¹⁴In quasi-one-dimension, one has for the width W of the wire $\lambda_F \ll W \ll L$, and W is smaller than, or comparable to, l_{el} .

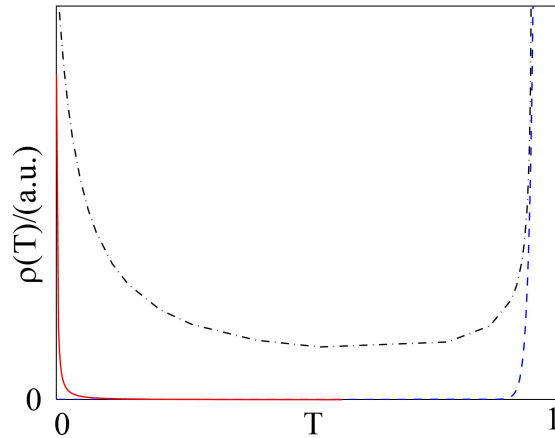


Figure 4.2: Transmission eigenvalue density $\rho(T)$ in ballistic (solid), diffusive (dash-dotted), and localized (dashed) regime.

The conventional DMPK equation applies to quasi-one-dimensional wires but generalizations for the equation have also been derived in higher dimensions [121, 122]. The present formulations of the DMPK equation, however, can not take into account nonequilibrium effects such as the reentrance effect (Subs. 2.3).

5 Scattering approach to quantum transport

The numerical scattering approach to quantum transport is a sort of numerical counterpart to the random matrix approach of Sec. 4. The scattering processes are described by the general scattering formalism of Subs. 4.1. Like the random matrix theory in normal metal systems, the numerical approach can be used to describe all the regimes, ballistic, diffusive, and localized, of transport. Further, the numerical approach applies also for normal-superconducting systems and finite voltages. The obvious drawback of this method is that it does not, per se, provide any interpretations, and the computations may become time consuming. In Papers III and IV the numerical scattering approach was adopted to study shot noise and thermoelectric effects.

In a similar way as for the random matrix theory, the idea of the numerical scattering approach is to calculate the quantity in question for many disorder "realizations". However, the expectation values are computed for some finite system with a finite number of realizations. Often the starting point is the tight-binding Hamiltonian of the scattering region

$$\begin{aligned}
 H = \sum_{\alpha=\pm 1} \alpha & \left[\sum_m \varepsilon_m |m, \alpha\rangle \langle m, \alpha| + \sum_{\langle m, n \rangle} (\gamma |n, \alpha\rangle \langle m, \alpha| + h.c.) \right] \\
 & + \sum_m [\Delta_{mm} |m, 1\rangle \langle m, -1| + h.c.], \tag{5.1}
 \end{aligned}$$

where only the interactions with neighbouring sites are included. Here m, n index the lattice site, $\langle m, n \rangle$ refers to the nearest neighbours, and α denotes the quasiparticle type ($\alpha = 1$ for an electron, $\alpha = -1$ for a hole). The disorder potential is modeled by generating random numbers or site energies ε_m from the range $[-w/2, w/2]$. The width of the disorder distribution also determines the mean free path l_{el} in the model. The superconducting pair potential is Δ_{ii} and γ is the nearest-neighbour coupling constant.

Because of the limited computational time, the conductors studied usually contain no more than some tens of thousands of lattice sites. In two dimensions, this corresponds to the width and length of the order of a few tens of nanometers. To

exclude possible finite-size effects one has to check that altering the size of the structure does not qualitatively change the results. The number of realizations needed to estimate certain quantity with a reasonable confidence interval depends on the distribution of the quantity. For conductance this is of the order of one hundred, whereas for shot noise thousands of realizations are usually needed. The retarded Green's function

$$\hat{G}^R = (E\hat{I} - \hat{H} - \hat{\Sigma}_L)^{-1} \quad (5.2)$$

takes into account the coupling of the scattering area to the semi-infinitely long ideal leads through the self-energy $\hat{\Sigma}_L$. This matrix inversion is the most time-consuming task in the algorithm. Originally, the matrix $\hat{H} + \hat{\Sigma}_L$ also contains information on the couplings of the sites inside the conductor. However, only the couplings between the leads are needed. Hence, for example, a so-called decimation method [123], which is essentially an efficient implementation of the Gaussian elimination method, may be used to exclude the excessive information.

From the Green's function G_{ji}^R connecting the leads i and j the scattering matrix is obtained using the Fisher-Lee relation [124]

$$s_{(j,b),(i,a)}^{\beta\alpha} = \delta_{(j,b),(i,a)}^{\beta\alpha} + i\hbar\sqrt{v_b^\beta v_a^\alpha} \langle b, \beta, j | G_{ji}^R | a, \alpha, i \rangle, \quad (5.3)$$

where v_a^α is the group velocity of the electrons ($\alpha = 1$) or holes ($\alpha = -1$) in mode a . Finally, the observables are expressed through scattering matrices and calculated from formulas similar to those in Sec. 4.1.

There is no permanent dividing line between the physical problems which are feasible for more analytical considerations and the ones which have to be solved mainly numerically. Generally, if it is possible to solve the transport problem at hand, e.g., through the quasiclassical approach, the random matrix theory, or the DMPK equation, these methods may be considered more convenient than the numerical scattering approach. In the absence of an analytical method the numerical scheme may prove useful. For the moment, the numerical scattering approach could be suitable to study, for example, the localization behavior of electronic states in the presence of the superconducting proximity effect.

6 Discussion

This Thesis considers quantum coherent phenomena from the point of view of mesoscopic fluctuations. The motivation for the studies of quantum coherence stems both from scientific and technological interest.

The role of quantum coherence in normal-metal structures is currently considered to be rather well understood, except for certain controversial topics. The one-parameter scaling hypothesis [36] may be considered as one of the fundamental principles in mesoscopic physics. It suggests, for example, that in an ensemble of mesoscopic wires, the behavior of conductance distribution is essentially described by a single scaling parameter, the dimensionless conductance g . In Paper I we calculated the corrections induced by the quantum interference effects, such as weak localization, on the conductance and current distributions in metallic wires. As long as noninteracting one-parameter scaling model is valid, the third and higher conductance cumulants are small with respect to unity. Actually, as was shown in Paper I, they are even smaller than previously thought. But noninteracting theory also provides a baseline for the study of interactions. In the measurements [29] that have spurred debate [38, 39], nonvanishing third and fourth conductance cumulants in low-conductance ($\sim 10 e^2/h$) metallic wires were observed. The authors of Ref. [29] suggest that the possible failure of the one-parameter scaling model in these experiments would be caused by electron-electron interactions. In another experiment, discrepancy has also been found when the mean free paths deduced from the magnetoresistance measurements and from the measurements of the time-dependent universal conductance fluctuations have been compared [40]. Typically, different parameters in mesoscopic structures are measured through conductance, the transport quantity easiest to detect. Generally, when feasible, it may be an interesting and nontrivial task to try to reconcile results obtained by conductance measurements and the outcome of the measurements of mesoscopic fluctuations. In the context of metallic disordered conductors, one can still mention one controversial topic: whether or not there exists electron dephasing at zero temperature. A widely recognized theory put forward in 1980s by Altshuler and Aronov [125] predicts a

diverging dephasing time at zero temperature, but in the experiments at low temperatures the dephasing rate seems to saturate to a finite value [21]. Presently, the part of the community involved in this question is divided into two camps. Roughly speaking, one group supports the aforementioned theory, and argues that, in one way or another, the dephasing observed in the experiments is caused by "external" sources or due to misinterpretation of the experiments [22, 126]. The other group holds the view that a finite dephasing rate is caused by more fundamental "intrinsic" mechanisms as suggested in a series of papers by Golubev and Zaikin [127–130].

In the presence of superconductivity, the calculations on the transport characteristics usually become more involved than in the normal-metal structures. For example, the localization-delocalization transition in normal-metal wires has been extensively studied by using random matrix theory and the DMPK equation [104, 131] but currently there is no counterpart for this equation for normal-superconducting systems at finite voltages. Despite the absence of an analytical scheme, the numerical scattering approach introduced in Sec. 5 could be applied to study localization behavior of the electronic states in the presence of the superconducting proximity effect.

The mesoscopic community has started to view current fluctuations, not as a distraction, but as a source of information. For example shot noise provides information not contained in conductance about different quantum coherent phenomena. Since the 1960s it has been known that a superconductor in good contact to a normal metal induces coherence of Andreev pairs to the latter. Shot noise measurements, or theoretical calculations, show that this superconducting proximity effect also brings about anticorrelations between the different Andreev pairs. Multiterminal structures, such as in Paper II, transmitting supercurrent, have been used to elucidate the role of the anticorrelation effect. In multiterminal structures it is feasible to control supercurrent by an external voltage. This is interesting also from a more device-oriented perspective since such structures make up a so-called π -junction [43] that bears relevance in the context of information processing applications, such as a superconducting transistor [41]. In a metallic wire in contact to a superconductor, the coherent quantum effects tend to surpass those in the absence of superconduct-

tivity. Besides supercurrent, this guideline is also exemplified by the reflectionless tunneling effect. This quantum interference effect may induce excess current and shot noise (Paper III) in NS structures at voltages much smaller than E_T/e . By measuring the differential conductance and shot noise through the structure at a certain voltage one can, for example, deduce the strength of the insulating barrier at the interface.

In recent years, besides charge transport, thermoelectric effects in normal-superconducting nanostructures have attracted attention [132–134]. Normal metals are good conductors of heat, compared, e.g., to superconductors. Further, the best conductors of electric current usually also carry heat well. This is summarized in the Wiedemann-Franz law, according to which the constant of proportionality between the thermal and electric conductivity linearly depends on temperature. Thermopower, however, measures the nonlinearities in the quasiparticle dispersion relation, and is small, of the order of T/E_F , in a normal metal. In the presence of superconductivity, Andreev reflection may induce deviations from the Wiedemann-Franz law [135] and Mott’s law (Paper IV).

Since the beginning of 1990s a prominent, still on-going, trend in condensed matter physics has been to consider different man-made analogies to the structures observed in nature. For example quantum dots, or so-called artificial atoms may serve as building blocks for future tunable solid-state lasers or nanoelectronic circuits. The Anderson atom model, originally put forward to describe magnetic impurities in a metal, applies also for the study of quantum dots and molecules [136, 137]. In Paper V we calculated the response functions of the exactly soluble Anderson atom model. This model for an isolated atom can be used as a reference point for more involved considerations.

In devices made out of metallic components, the nature of transport is typically diffusive, and the operation frequency is limited by the Thouless energy $E_T = D/L^2$, or the diffusion constant D and the characteristic length L . The carbon structures, e.g., graphene, allow ballistic transport and, therefore, potentially faster operation of devices. In fabrication technologies, there is an incessant quest for cleaner materials, and integration of smaller elements into larger circuits. From the technological, and

even commercial point of view, solid state structures are intriguing since they allow for scalability and integration to larger circuits. As an example, the existence of nonclassical correlations, entanglement, between particles is at the heart of quantum information. Such correlations, which may manifest themselves as a breaking of Bell inequality, have recently been detected in noise correlation measurements, e.g., in a solid state analogy of a Hanbury Brown Twiss geometry, a setup familiar from optics since the 1950s [138]. Controlling entanglement in the nanocircuits including large numbers of quantum bits is one of the great challenges in the field of quantum computing.

Mesoscopic physics is progressing, but the direction of the development is to some degree unpredictable. Mesoscale conductors are a realistic and promising platform for making practical use of quantum coherence.

References

- [1] R. P. Feynman and A. R. Hibbs, *Quantum Mechanics and Path Integrals* (McGraw-Hill, New York, 1965).
- [2] P. A. Lee and T. V. Ramakrishnan, *Rev. Mod. Phys.* **57**, 287 (1985).
- [3] J. Rammer, *Rev. Mod. Phys.* **63**, 781 (1991).
- [4] A. A. Abrikosov, L. P. Gorkov, and I.E. Dzyaloshinski, *Methods of Quantum Field Theory in Statistical Physics* (Dover Publications, Inc., New York, 1975).
- [5] A. L. Fetter and J. D. Walecka, *Quantum Theory of Many-Particle Systems* (McGraw-Hill, New York, 1971).
- [6] G. D. Mahan, *Many-Particle Physics* (Plenum Press, New York, 1990).
- [7] P. G. de Gennes, *Superconductivity of Metals and Alloys* (W. A. Benjamin, New York, 1966).
- [8] M. Tinkham, *Introduction to Superconductivity*, 2nd ed. (McGraw-Hill, Singapore 1996).
- [9] J. R. Schrieffer, *Theory of Superconductivity*, revised ed., Advanced Book Program, (Westview Press, Boulder Colorado, 1999).
- [10] J. B. Ketterson and S. N. Song, *Superconductivity* (University Press, Cambridge, 1999).
- [11] S. Datta, *Electronic Transport in Mesoscopic Systems* (Cambridge University Press, Cambridge, 1995).
- [12] J. Rammer, *Quantum Transport Theory*, (Perseus Books, Massachusetts, 1998).
- [13] B. D. Simons and A. Altland, *Theories of Mesoscopic Physics, in CRM Summer School Theoretical Physics at the End of the 20th Century*, CRM Series in Mathematical Physics (Springer, Berlin, 2000).

- [14] D. Mailly and M. Sanquer, *J. Phys. (France) I* **2**, 357 (1992).
- [15] R. Landauer, *Philos. Mag.* **21**, 863 (1970).
- [16] A. Stern, Y. Aharonov, and Y. Imry, *Phys. Rev. A* **41**, 3436 (1990).
- [17] M. Sigrist, T. Ihn, K. Ensslin, D. Loss, M. Reinwald, and W. Wegscheider, *Phys. Rev. Lett.* **96**, 036804 (2006).
- [18] D. M. Pooke, N. Paquin, M. Pepper, and A. Gundlach, *J. Phys.: Condens. Matter* **1**, 3289 (1989).
- [19] T. Hiramoto, K. Hirakawa, Y. Iye, and T. Ikoma, *Appl. Phys. Lett.* **54**, 2103 (1989).
- [20] R. M. Mueller, R. Stasch, and G. Bergmann, *Solid State Commun.* **91**, 255 (1994).
- [21] P. Mohanty, E. M. Q. Jariwala, and R. A. Webb, *Phys. Rev. Lett.* **78**, 3366 (1997).
- [22] F. Pierre, A. B. Gougam, A. Anthore, H. Pothier, D. Esteve, and N. O. Birge, *Phys. Rev. B* **68**, 085413 (2003).
- [23] F. Schopfer, C. Bäuerle, W. Rabaud, and L. Saminadayar, *Phys. Rev. Lett.* **90**, 056801 (2003).
- [24] F. Mallet, J. Ericsson, D. Mailly, S. Ünlübayir, D. Reuter, A. Melnikov, A. D. Wieck, T. Micklitz, A. Rosch, T. A. Costi, L. Saminadayar, and C. Bäuerle, *Phys. Rev. Lett.* **97**, 226804 (2006).
- [25] G. K. White, *Experimental Techniques in Low-Temperature Physics*, 4th edition (Oxford University Press, New York, 2002).
- [26] R. H. Baughman, A. A. Zakhidov, and W. A. de Heer, *Science* **297**, 787 (2002).
- [27] K. S. Novoselov, A. K. Geim, S. V. Morozov, D. Jiang, Y. Zhang, S. V. Dubonos, I. V. Grigorieva, and A. A. Firsov, *Science* **306**, 666 (2004).

- [28] S. Hikami, A. I. Larkin, and Y. Nagaoka, *Prog. Theor. Phys.* **63**, 707 (1980).
- [29] P. Mohanty and R. A. Webb, *Phys. Rev. Lett.* **88**, 146601 (2002).
- [30] B. Reulet, J. Senzier, and D. E. Prober, *Phys. Rev. Lett.* **91**, 196601 (2003).
- [31] Yu. Bomze, G. Gershon, D. Shovkun, L. S. Levitov, and M. Reznikov, *Phys. Rev. Lett.* **95**, 176601 (2005).
- [32] S. Gustavsson, R. Leturcq, B. Simovic, R. Schleser, T. Ihn, P. Studerus, K. Ensslin, D. C. Driscoll, and A. C. Gossard, *Phys. Rev. Lett.* **96**, 076605 (2006).
- [33] E. V. Sukhorukov, A. N. Jordan, S. Gustavsson, R. Leturcq, T. Ihn, and K. Ensslin, *Nature Physics* **3**, 243 (2007).
- [34] A.V. Timofeev, M. Meschke, T. Peltonen, T.T. Heikkilä, and J.P. Pekola, *Phys. Rev. Lett.* **98**, 207001 (2007).
- [35] H. Smith and H. H. Jensen, *Transport Phenomena* (Clarendon, Oxford, 1989).
- [36] E. Abrahams, P. W. Anderson, D. C. Licciardello, and T. V. Ramakrishnan, *Phys. Rev. Lett.* **42**, 673 (1979).
- [37] B. L. Altshuler, V. E. Kravtsov and I. V. Lerner, *Zh. Eksp. Teor. Fiz.* **91**, 2276 (1986) [*Sov. Phys. JETP* **64**, 1352 (1986)].
- [38] O. Tsypliyatyev, I. L. Aleiner, V. I. Fal'ko, and I. V. Lerner, *Phys. Rev. B* **68**, 121301 (2003).
- [39] P. Mohanty and R. A. Webb, *Phys. Rev. Lett.* **93**, 159702 (2004).
- [40] A. Trionfi, S. Lee, and D. Natelson, *Phys. Rev. B* **75**, 104202 (2007).
- [41] F. K. Wilhelm, G. Schön, and A. D. Zaikin, *Phys. Rev. Lett.* **81**, 1682 (1998).
- [42] V. T. Petrashov, K. G. Chua, K. M. Marshall, R. Sh. Shaikhaidarov, and J. T. Nicholls, *Phys. Rev. Lett.* **95**, 147001 (2005).

- [43] J.J.A. Baselmans, A.F. Morpurgo, B.J. van Wees, and T.M. Klapwijk, *Nature* (London) **397**, 43 (1999).
- [44] J. Huang, F. Pierre, T. T. Heikkilä, F. K. Wilhelm, and N. O. Birge, *Phys. Rev. B* **66**, 020507 (2002).
- [45] N. W. Ashcroft and A. D. Mermin, *Solid State Physics* (Saunders College Publishing, Orlando, 1976).
- [46] C. P. Poole, *Handbook of Superconductivity* (Academic Press, San Diego, 2000).
- [47] N. Nagaosa and S. Heusler, *Quantum Field Theory in Condensed Matter Physics* (Springer, Berlin, 1999).
- [48] B. D. Josephson, *Phys. Lett.* **1**, 251 (1962).
- [49] K. K. Likharev, *Rev. Mod. Phys* **51**, 101 (1979).
- [50] F. K. Wilhelm, A. D. Zaikin, and G. Schön, *J. Low Temp. Phys.* **106**, 305 (1997).
- [51] T. T. Heikkilä, J. Särkkä, and F. K. Wilhelm, *Phys. Rev. B* **66**, 184513 (2002).
- [52] D. Averin and H. T. Imam, *Phys. Rev. Lett.* **76**, 3814 (1996).
- [53] A. F. Andreev, *Sov. Phys. JETP.* **19**, 1228 (1964).
- [54] A. M. Zagoskin, *Quantum Theory of Many-Body Systems: Techniques and Applications* (Springer, New York, 2004).
- [55] W. L. McMillan, *Phys. Rev.* **175**, 559 (1968).
- [56] M. J. M. de Jong and C. W. J. Beenakker, *Phys. Rev. B* **49**, 16070 (1994).
- [57] B. J. van Wees, P. de Vries, P. Magnée, and T. M. Klapwijk, *Phys. Rev. Lett.* **69**, 510 (1992).

- [58] F. W. J. Hekking and Y. V. Nazarov, *Phys. Rev. B* **49**, 6847 (1994).
- [59] R. J. Elliott, *Phys. Rev.* **96**, 266 (1954).
- [60] G. Bergmann, *Phys. Rev. Lett.* **48**, 1046 (1982).
- [61] G. Bergmann, *Phys. Rep.* **107**, 1 (1984).
- [62] P. A. Mello, *Phys. Rev. Lett.* **60**, 1089 (1988).
- [63] P. A. Mello and A. D. Stone, *Phys. Rev. B* **44**, 3559 (1991).
- [64] A. M. S. Macêdo and J. T. Chalker, *Phys. Rev. B* **46**, 14985 (1992).
- [65] C. P. Umbach, S. Washburn, R. B. Laibowitz, and R. A. Webb, *Phys. Rev. B* **30**, 4048 (1984).
- [66] J. C. Licini, D. J. Bishop, M. A. Kastner, and J. Melngailis, *Phys. Rev. Lett.* **55**, 2987 (1985).
- [67] K. B. Efetov and A. I. Larkin, *Zh. Eksp. Teor. Fiz.* **85**, 764 (1983) [*Sov. Phys. JETP* **58**, 444 (1983)].
- [68] P. A. Mello and J.-L. Pichard, *Phys. Rev. B* **40**, 5276 (1989).
- [69] C. W. J. Beenakker, *Phys. Rev. B* **49**, 2205 (1994).
- [70] W. Schottky, *Ann. Phys. (Leipzig)* **57**, 541 (1918).
- [71] C. W. J. Beenakker and M. Büttiker, *Phys. Rev. B* **46**, 1889 (1992).
- [72] W. Belzig, F. K. Wilhelm, C. Bruder, G. Schön, and A. D. Zaikin, *Superlatt. Microstruct.* **25**, 1251 (1999).
- [73] M. Houzet and F. Pistoiesi, *Phys. Rev. Lett.* **92**, 107004 (2004).
- [74] L. D. Landau, *Sov. Phys. JETP.* **3**, 920 (1957).
- [75] L. D. Landau, *Sov. Phys. JETP.* **5**, 101 (1957).

- [76] P. Nozières, *Theory of Interacting Fermi Systems* (Benjamin, New York, 1964).
- [77] Y. Nambu, Phys. Rev. **117**, 648 (1960).
- [78] J. Rammer and H. Smith, Rev. Mod. Phys. **58**, 323 (1986).
- [79] A. Kamenev in *Nanophysics: Coherence and Transport, Les Houches session LXXXI*, edited by H. Bouchiat, Y. Gefen, S. Guéron, G. Montambaux, and J. Dalibard, NATO ASI (Elsevier, Amsterdam, 2005), p.177.
- [80] L. P. Gorkov, JETP **7**, 505 (1958).
- [81] C. J. Lambert and R. Raimondi, J. Phys. Condens. Matter **10**, 901 (1998).
- [82] N. Kopnin, *Theory of Nonequilibrium Superconductivity*, (Clarendon, Oxford, 2001).
- [83] V. Chandrasekhar in *The Physics of Superconductors*, Vol II, edited by K. H. Bennemann and J. B. Ketterson (Springer, New, York, 2004), p. 55.
- [84] G. Eilenberger, Z. Phys. **214**, 195 (1968).
- [85] Y. V. Nazarov, Superlattices Microstruct. **25**, 1221 (1999).
- [86] P. Virtanen and T. T. Heikkilä, J. Low Temp. Phys. **136**, 401 (2005).
- [87] H. Pothier, S. Guéron, N. O. Birge, D. Esteve, and M. H. Devoret, Phys. Rev. Lett. **79**, 3490 (1997).
- [88] Yu. V. Nazarov, Ann. Phys. (Berlin) **8**, SI-193 (1999).
- [89] L. S. Levitov, in *Quantum Noise in Mesoscopic Physics*, edited by Yu. V. Nazarov (Kluwer, Dordrecht, 2003), p. 373.
- [90] W. Belzig, in *Quantum Noise in Mesoscopic Physics*, edited by Yu. V. Nazarov (Kluwer, Dordrecht, 2003), p. 463.
- [91] M. Kindermann, *Electron Counting Statistics in Nanostructures* (Ph.D. Thesis, University of Leiden, the Netherlands, 2003).

- [92] Y. V. Nazarov and D. A. Bagrets, *Phys. Rev. Lett.* **88**, 196801 (2002).
- [93] X. Jehl, M. Sanquer, R. Calemczuk, and D. Mailly, *Nature (London)* **405**, 50 (2000).
- [94] A. A. Kozhevnikov, R. J. Schoelkopf, and D. E. Prober, *Phys. Rev. Lett.* **84**, 3398 (2000).
- [95] F. Lefloch, C. Hoffmann, M. Sanquer, and D. Quirion, *Phys. Rev. Lett.* **90**, 067002 (2003).
- [96] B. Reulet, A. A. Kozhevnikov, D. E. Prober, W. Belzig, and Y. V. Nazarov, *Phys. Rev. Lett.* **90**, 066601 (2003).
- [97] W. Belzig and Y. V. Nazarov, *Phys. Rev. Lett.* **87**, 067006 (2001).
- [98] P. Samuelsson and M. Büttiker, *Phys. Rev. B* **66**, 201306 (2002).
- [99] W. Belzig and P. Samuelsson, *Europhys. Lett.* **64**, 253 (2003).
- [100] P. Virtanen and T. T. Heikkilä, *New J. Phys.* **8**, 50 (2006).
- [101] E. V. Bezuglyi, E. N. Bratus', V. S. Shumeiko, and V. Vinokur, *Phys. Rev. B* **70**, 064507 (2004).
- [102] M. Büttiker, *Phys. Rev. Lett.* **65**, 2901 (1990).
- [103] P. A. Mello, P. Pereyra, and N. Kumar, *Ann. Phys., NY* **181**, 290 (1981).
- [104] C. W. J. Beenakker, *Rev. Mod. Phys.* **69**, 731 (1997).
- [105] C. W. J. Beenakker, *Phys. Rev. B* **47**, 15763 (1993).
- [106] P. W. Brouwer, *On the Random-Matrix Theory of Quantum Transport* (Ph.D. Thesis, University of Leiden, the Netherlands, 1997).
- [107] T. Guhr, A. Müller-Groeling, and H. A. Weidenmüller, *Phys. Rep.* **299**, 189 (1998).
- [108] M. L. Mehta, *Random Matrices* (Academic Press, New York, 2004).

- [109] K. B. Efetov in *Applications of Random Matrices in Physics*, edited by É. Brezin, V. Kazakov, D. Serban, P. Wiegmann, and A. Zabrodin (Springer, Dordrecht, 2006), p. 95.
- [110] P. Heinzner, A. Huckleberry, and M. R. Zirnbauer, *Commun. Math. Phys.* **257**, 725 (2005).
- [111] A. Altland and M. R. Zirnbauer, *Phys. Rev. Lett.* **76**, 3420 (1996).
- [112] A. Altland and M. R. Zirnbauer, *Phys. Rev. B* **55**, 1142 (1997).
- [113] P. W. Brouwer, C. Mudry, B. D. Simons, and A. Altland, *Phys. Rev. Lett.* **81**, 862 (1998).
- [114] P. W. Brouwer, A. Furusaki, I. A. Gruzberg, and C. Mudry, *Phys. Rev. Lett.* **85**, 1064 (2000).
- [115] P. A. Mello and N. Kumar, *Quantum Transport in Mesoscopic Systems: Complexity and Statistical Fluctuations* (Oxford University Press, New York, 2004).
- [116] C. E. Shannon, *Bell Syst. Tech. J.* **27**, 379 (1948).
- [117] M. Gaudin and P. A. Mello, *J. Phys. G: Nucl. Phys.* **7**, 1085 (1981).
- [118] K. A. Muttalib and J. R. Klauder, *Phys. Rev. Lett.* **82**, 4272 (1999).
- [119] O. N. Dorokhov, *Pis'ma Zh. Eksp. Teor. Fiz.* **36**, 259 (1982) [*JETP Lett.* **36**, 318 (1982)].
- [120] P. A. Mello, *J. Math. Phys. (N.Y.)* **27**, 2876 (1986).
- [121] K. A. Muttalib and V. A. Gopar, *Phys. Rev. B* **66**, 115318 (2002).
- [122] P. Shukla and I. P. Batra, *Phys. Rev. B* **71**, 235107 (2005).
- [123] M. Leadbeater and C. J. Lambert, *Ann. der Phys.* **7**, 498 (1998).
- [124] D. S. Fisher and P. A. Lee, *Phys. Rev. B* **23**, 6851 (1981).

- [125] B. L. Altshuler and A. G. Aronov, in *Electron-Electron Interactions in Disordered Systems*, edited by A. L. Efros and M. Pollak (Elsevier, Amsterdam, 1985).
- [126] F. Pierre and N. O. Birge, *Phys. Rev. Lett.* **89**, 206804 (2002).
- [127] D. S. Golubev and A. D. Zaikin, *Phys. Rev. Lett.* **81**, 1074 (1998).
- [128] D. S. Golubev and A. D. Zaikin, *Phys. Rev. B* **59**, 9195 (1999).
- [129] D. S. Golubev and A. D. Zaikin, *Phys. Rev. B* **62**, 14061 (2000).
- [130] D. S. Golubev and A. D. Zaikin, *J. Low Temp. Phys.* **132**, 11 (2003).
- [131] K. A. Muttalib, P. Wölfle, and V. A. Gopar, *Ann. Phys.* **308**, 156 (2003).
- [132] J. Eom, C.-J. Chien, and V. Chandrasekhar, *Phys. Rev. Lett.* **81**, 437 (1998).
- [133] E. V. Bezuglyi and V. Vinokur, *Phys. Rev. Lett.* **91**, 137002 (2003).
- [134] Z. Jiang and V. Chandrasekhar, *Phys. Rev. Lett.* **94**, 147002 (2005).
- [135] N. R. Claughton and C. J. Lambert, *Phys. Rev. B* **53**, 6605 (1996).
- [136] N. H. Bondaeo, J. Erland, D. Gammon, D. Park, D. S. Katzer, and D. G. Steel, *Science* **282**, 1473 (1998).
- [137] J. Koch, M. E. Raikh, and F. von Oppen, *Phys. Rev. Lett.* **96**, 056803 (2006).
- [138] R. Hanbury-Brown and R. Q. Twiss, *Philos. Mag.* **45**, 663 (1954).